VARIATION OF POSITRONIUM τ_2 LIFETIME WITH TEMPERATURE

--ELECTRONIC SYSTEM OF MEASUREMENT

By

JAMES LINVILLE PIGG

Bachelor of Arts

Linfield College

McMinnville, Oregon

1959

Submitted to the Faculty of the Graduate School of
the Oklahoma State University
in partial fulfillment of the requirements
for the degree of
MASTER OF SCIENCE
May, 1962

VARIATION OF POSITRONIUM τ_2 LIFETIME WITH TEMPERATURE

--ELECTRONIC SYSTEM OF MEASUREMENT

Thesis Approved:

B. Clark Groseclose
Thesis Adviser

H. G. Harrington

Robert MacVicar
Dean of the Graduate School

PREFACE

A positron, under certain conditions, may capture an electron to form a quasi-stable system called the positronium atom. The annihilation radiation of these pairs promises to serve as an investigation tool for the energetics and structure of the positronium's environment. Many theoretical questions remain unanswered for lack of more complete experimental data. It is hoped that these studies contribute toward understanding more fully these phenomena.

During the course of this work Dr. B. Clark Groseclose contributed invaluable assistance and guidance, for which I am sincerely grateful. I should also like to express my thanks to my colleagues Robert Eagleton and Gerald Loper for their cooperation during this work. I should further like to thank Benard Sodek and Jon Ables for the computer time and assistance they gave me. I should further like to acknowledge the machine shop personnel--Heinz Hall, Richard Gruelke, and Frank Hargrove--for their work.

The author was supported by an N.D.E.A. Fellowship while in the Oklahoma State University Graduate School.

TABLE OF CONTENTS

LIST OF TABLES

LIST OF FIGURES

CHAPTER I

INTRODUCTION

The discovery that the decay rate of annihilating positrons in a gas medium is not proportional to the gas pressure as predicted by the Dirac Theory[1] led many investigators to the study of various aspects of positron annihilation. Shearer and Deutsch[2] suggested that the results of their experiment could be explained if some of the positrons were annihilating from a bound system. If such were the case, the conditions favoring annihilation would be independent of pressure. This bound system was supposed to be the "positronium atom" which had been previously discussed by Wheeler[3] and Pirenne.[4] Pond[5] then calculated that between 1/4 and 1/3 of all positrons joined with an electron to form this bound system in most gases. When the electron and positron form a bound state, they may join with their spins aligned parallel or anti-parallel. The first case is the triplet ^3S state, called orthopositronium, while the latter is the singlet ^1S state called parapositronium.

Ore and Powell[6] predicted that parapositronium would have a life-time of 1.25×10^{-10} sec and then decay by two quanta emission, while the orthopositronium would annihilate via three gamma rays in 1.4×10^{-7} seconds. Subsequent experiments verified this picture and their orders of magnitude.[7,8]

Bell and Graham[9] and de Benedetti and Ritchings[10] then investigated positron annihilation in solids with the following results: 1) In metals,

ionic crystals, and valence crystals, there was a single lifetime which was surprisingly constant from material to material; 2) In organic materials, amorphous solids, and plastics, two lifetimes were observed. The second lifetime accounted for about 30% of the decays.

There are four stages of the positron's life which are important in lifetime measurements. The first step is its ejection from a positron emitting radioiosotope, which is Na^{22} in this experiment. Almost immediately after the positron is ejected from the sodium nucleus, a 1.28 Mev gamma ray is emitted. The positron then slows down to thermal energies very rapidly and may then unite with an electron to form a bound system. The final stage for the positron is its mutual annihilation with an electron in which two 0.51 Mev photons are created. Thus, by measuring the time difference between the 1.28 Mev "birth announcement" and the 0.51 Mev annihilation gamma, one can obtain the lifetime of the positron. Considering only the positrons which do join an electron in a bound system, or "positronium atom," the measurement would give the positronium lifetime if the first two phases of the positrons existence are negligibly short in comparison to the time it is engaged in the bound system. Accordingly, evidence to show that the 1.28 Mev gamma ray is emitted in a time many orders of magnitude smaller than the positrons lifetime and that, likewise, thermalization occurs in a negligible fraction of the positronium lifetime shall now be presented.

A. Decay of Sodium 22

The Na^{22} positron emitter has a half-life of 2.6 years and offers a suitable source for life-time measurements. It has the decay scheme

shown in Figure 1 as determined by Hinman, Brower, and Leamer.[11] Transitions to the ground state usually take place by means of electric quadrupole radiation.

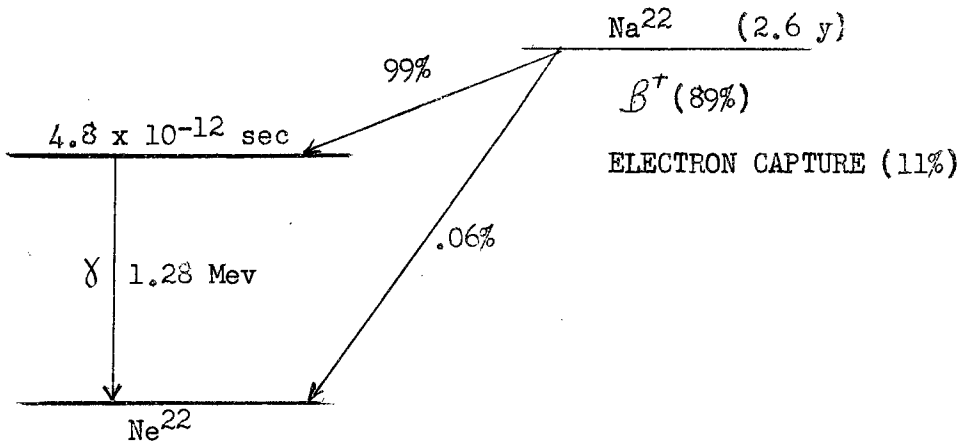

Figure 1. Sodium-22 Decay Schemes

From theoretical considerations, Weisskopf[12] and Moszkowski[13] have predicted a lifetime in the excited state on the order of a few times 10^{-11} seconds. Sunyar,[14] however, points out that theoretical estimates of the E2 transition probabilities are usually too low by considerable factors in decays which have been measured. Hence, the lifetime might very well be less than 10^{-11} seconds. Although pulse electronics have not sufficiently evolved for a direct measurement, an indirect experimental figure was obtained for the lifetime of the 1.28 excited level by Alkhazov et al.[15] by measuring the Coulomb excitation cross-section for this state. In this way, the reduced transition probability, and hence the lifetime (which is the reciprocal of the transition probability) of the radiative transition was calculated.

The lifetime value estimated was 4.8×10^{-12} seconds for the 1.28 Mev. level of Ne^{22}.

The implications of this work are, of course, that the 1.28 Mev. gamma ray may be considered prompt with respect to the ejection of the positron in so far as the lifetime of the positron is concerned.

B. Thermalization

The thermalization time in metals was first calculated by de Benedetti et al.[16] to be about 3×10^{-10} seconds on the basis of energy loss of the positrons as they go through the successive stages of exciting or ionizing the atoms of the absorber, then by causing inter-band electronic transitions, and eventually, when the energy is too low for this, by excitation of lattice vibrations. Garwin[17] modified these calculations to include another mechanism, that of the positron energy loss involved in the Coulomb scattering of conduction electrons whereby the electrons are increased in energy and scattered out of the Fermi sea. He estimated the thermalization time should be much shorter--about 10^{-14} seconds. Lee-Whiting[18] refined Garwin's computations and removed some of the crude approximations to obtain the presently accepted value of 3×10^{-12} seconds. Since this is significantly smaller than the lifetime, we conclude that positrons in metals are completely thermalized upon annihilation.

The slowing-down process is much more complicated for insulators when the positron is no longer energetic enough to promote electrons into an excited band, although the initial stages of the slowing-down process again proceed very rapidly. Once the energy reaches the electron volt region, the positron velocity becomes comparable with the velocities

of the outer-shell electrons of the molecule, and the cross section for formation of positronium becomes of the order of magnitude of atomic dimensions.[16] The cross section for the loss of an electron by positronium is of the same order of magnitude. Consequently, the positron can be expected to capture and lose electrons continually in this energy range. This will cease when the energy becomes sufficiently low that these processes are no longer possible energetically. Experimentally, there is also good reason for assuming that positrons are slowed down to thermal energies. DuMond et al.[19] measured the center of mass velocity of the annihilating pair using a gamma ray spectrometer. Other experimenters[20,21] corroborated his results that the momentum of the annihilating pair is about mc/137, corresponding to a v/c figure of about 4×10^{-3} and an energy on the order of 16 electron volts. Thus, most of the positrons are thermalized before annihilation.

Annihilation in flight studies give further evidence that a great majority of positrons will be annihilated at low energies. Heitler[22] calculated that the probability that a positron is annihilated while in flight is only 2% for 500Kev positrons. Although annihilations in flight have been observed by Deutsch[23] and Gerhart,[24] the probability of such an event occuring is considerably smaller than the probability of the annihilation of positrons in thermal equilibrium.[17,25]

C. Evidence of Positronium Formation

de Benedetti and co-workers[16] proposed that after thermalization, the positrons diffuse freely through the lattice until annihilation. The first experiment to test this proposal was conducted by Madansky and Rasetti[25] in 1950. Assuming this point of view, they attempted to

measure slow positrons' diffusion length by collecting the positrons on a negatively charged electrode as they emerged from a metal surface. The results were clearly negative so the possibility that the positrons were captured in bound states arose. A second test was applied by de Benedetti and Siegel[26] in an experiment which measured the σ_3/σ_2 ratio.

The ratio of the three-quantum to two-quantum annihilation rate is given in the theory to be $\frac{\sigma_3}{\sigma_2} = \frac{1}{1115}$ (see next chapter). However, for spins distributed at random we have three parapositronium atoms for every positronium atom, thus $\frac{3\sigma_3}{\sigma_2} = \frac{1}{373}$. On the other hand, if positronium is formed the electron spins tend to become aligned with the positron spins so that more three quantum annihilation would be expected due to the formation and decay of orthopositronium. Their experiments yielded the results that in gases, the σ_3/σ_2 of 30% indicates formation of positronium. In aluminum and some non-conducting liquids, however, they obtained the $\frac{1}{373}$ value expected for random statistical distribution.

Thus, if orthopositronium is formed, rapid conversions from the ortho to the para states resulting from exchange collisions with electrons quenches the triplet state and re-establishes statistical equilibrium.

The idea of positronium formation was further substantiated by Bell and Graham's work on positronium mean lives in condensed material.[9] It will be shown in the next chapter that if the positrons annihilate in free collisions, the upper and lower limits on the mean lives of positions in some alkali metals are

	Li	K	Cs
τ_{max}	29	102	160
τ_{min}	1.7	4.2	5.6

where τ is measured in 10^{-10} seconds.

From this it is seen that the positron mean life should be at least 2.5×10^{-10} seconds longer in K than in Li. However, comparison measurements by de Benedetti and Ritchings[10] showed that not only in K and Li but also in Na, Ag, Pb, Cu, C, S, and a few salts, the mean lives were the same within 0.5×10^{-10} seconds. These results were corroborated by Bell and Graham's absolute measurements which showed that all one- and two-electron metals produce mean lives between 1.2 and 1.7×10^{-10} seconds.

D. Anamolous τ_2 Component in Metals

Several workers[9,27,28] have found evidence for believing that an anomalous τ_2 component exists, but treated the problem lightly as the τ_2 values lie beyond the instrumental resolution. Recently, however, Bell and Jorgensen[29] confidently reported the τ_2 in low abundance in aluminum ($\tau_2 = 3.85 \times 10^{-10}$ sec., I = 6.5%), lithium ($\tau_2 = 5.9 \times 10^{-10}$ sec., I = 6.5%), and sodium ($\tau_2 = 5.7 \times 10^{-10}$ sec., I = 4.3%). These results still lack theoretical explanation.

E. Annihilation in Amorphous Solids

The annihilation of positrons in many solid materials is complicated by the fact that a number of competing processes may occur. Such a situation occurs in the amorphous solids in which there are two components of the lifetime, a "long" component between a half and ten millimicroseconds, and a "short" component which is a fraction of this time. The long component is attributed to the formation of orthopositronium as this system, when unmolested, has a lifetime of about one hundred millimicroseconds.

The annihilation of a positron with a electron can theoretically emit any number of photons with the reservation that the probability of such annihilations decreases by order α (where α is the fine structure constant, 1/137) for each additional photon characterizing the decay. Only annihilations involving one, two, and three photons have been observed in practice. Single photon annihilation can occur when a third agent is available to carry away the excess momentum. Thus, this process can occur when a positron annihilates with an electron bound to a nucleus, the nucleus recoiling to conserve linear momentum. According to Heitler,[22] this process is proportional to the fifth power of the atomic number of the absorber. However, even in lead, which has a maximum cross section at an energy of 10 mc^2, the maximum cross section of one photon annihilation is only 20% of the two photon cross section and this cross section has a monotonic decrease for decreasing energy. Consequently, the relative abundance of single quantum annihilation is negligible during the absorption of positrons emitted by radioactive sources like Na^{22}. Thus, two or more quanta will accompany positron annihilation from both free electron and bound state annihilation. The long lifetime component of positronium annihilation in amorphous substances, however, has a much shorter value than the lifetime figure obtained from theoretical considerations of the isolated orthopositronium system. This lifetime varies with temperature and composition of the absorber and is characterized by two photon decay.

The observation that the long lifetime component is much shorter than the theoretical value can be explained by the mechanism of ortho- to parapositronium conversion, which depopulates the triplet level in favor of the rapid decaying singlet level. Triplet to singlet conversion

can result from "pickoff" annihilation in which the positron annihilates with a neighboring electron in the lattice. In certain materials a collision can also induce an actual exchange between the electron in the positronium atom and an electron of opposite spin from a neighboring atom. In order to effect an electron exchange, the neighboring atom must have two closely spaced energy levels of opposite spin (one of which is vacant) and the positronium atom must furnish an amount of energy equal to this difference in levels. Suitable conversion (or, more commonly called "quenching") agents are those whose energy level spacing is of the order of thermal energies. Free electrons in a conductor by virtue of the high concentration should provide a high triplet to singlet conversion of positronium. Magnetic fields, by mixing the singlet and triplet states, can also hasten the destruction of positronium.

F. Annihilation in Liquids

The annihilation of positrons in liquids follows the same general pattern as in amorphous solids with respect to the complex decay mode and the resulting relative intensities. The long lived component in most organic liquids and water lies between one and two millimicroseconds and accounts for from 20 to 30 percent of the total annihilations. Berko and Zuchelli[30] found that the lifetime of the long component could be altered by inserting small amounts of a suitable "quenching" agent in the liquid. The intensities remained constant, however, as might be expected. Such experiments are performed by adding a paramagnetic free radical such as diphenyl picryl hydrazyl, which makes conditions favorable for the spin exchange collision mechanism with the unpaired electron of the free radical. The exchange cross sections are of the

order of 10^{-17} cm^2 which is the same order of magnitude as the triplet quenching cross section in gases due to the addition of NO.[31]

Green and Bell[27] have also found it possible to quench the intensity without appreciably affecting the lifetime by adding either NO_2^- or NO_3^- ions to water. This process is interpreted as a decrease in the number of positrons available for positronium formation due to the capture of some of the positrons by the negative ions to form the chemical compounds positronium nitrate or nitrite. These captured positrons then decay with a short lifetime in a similar manner to those annihilating from a singlet state.

G. Annihilation in Gases

The annihilation of positrons in gases is quite similar to the corresponding process in liquids and amorphous solids. Dulit, Gittleman, and Deutsch[32] studied the relative rates of two- and three-quantum decay in gases. Their results indicated that the relative number of positrons which go into the bound state generally is between 33% (argon) and 40% (freon). These results assume that three-fourths of the positrons which form positronium decay with three-gamma annihilation as predicted in the theory. These limits are similar to those in amorphous solids. The main difference, arising from the greatly reduced density of gases, is that the free annihilation cross section which is dependent on the electron density is greatly reduced, resulting in a quite longer lifetime for annihilation by direct collision. A short period, of the order of the slowing down time of the positrons, has been detected, but not measured with significant accuracy. This mode of decay was interpreted as annihilation from the short-lived state, parapositronium. A second

period, of the order of magnitude of that predicted by the Dirac cross section and inversely dependent on the gas pressure, is strongly suggestive of annihilation of the positron during free collisions with the atomic electrons. The third period is practically independent of pressure and corresponds to a mean life of about 0.14 microseconds, which is consistent with a model based on annihilation from orthopositronium atoms. The fact that the three photon yield is much increased in those gases which are characterized by a relatively intense, pressure independent, long lifetime component is further evidence for this interpretation.

In gases also, it is found possible to quench the longer lifetimes; vix. NO, NO_2, and the halogens. The quenching process due to NO was explained by Deutsch in terms of a spin flip due to electron exchange during collisions between the bound positronium positron and the unpaired electron of the NO molecule. The quenching effect of the halogen molecules, however, was interpreted in terms of a formation of chemical compounds between the positrons (positive positronium ions) and the halogen ions. The spin exchange mechanism results in a shortening of the lifetime of the orthopositronium, the amount of the shortening depending on the concentration of the quenching material, without significantly altering the intensity of the component. The two photon decay rate should also rise at the expense of the three photon rate as the concentration of the quenching agent was increased. Quenching by chemical compound formation, on the other hand, would tend to alter the intensity of the long lived component rather than the value of the lifetime, the reduction being dependent on the concentration of the quenching agent. This mechanism is the same as that postulated by Green and Bell[27] to explain their observations of such effects in liquids.

H. One-Gamma Annihilation

Single-quantum annihilation was observed by Whalen[33] using the following technique. Positrons emitted from Na^{22} and energy selected by a thin-lens beta ray spectrometer impinge upon and stop in a 107-mg/cm lead foil. A two inch thick scintillation crystal detects the single quantum annihilation photons, and a 1-mm crystal directly behind the stopping foil detects the K_α x-rays which follow the annihilation of the K-shell electrons in the lead. A single-quantum annihilation event appears as a coincidence between the outputs of the two scintillation spectrometers, both of which employ differential energy discrimination. Substitution of Al foil as the positron stopper affords the measurement of the background coincidence rate. The results for lead and uranium agree with the theoretical predictions.[34]

I. Angular Correlation Experiments

Another family of experiments of interest in the investigation of positron annihilation is that of angular correlation. From this work one may obtain information pertaining to the state of the system prior to annihilation and the σ_3/σ_2 ratio.

1. Two Gamma Annihilation

Upon annihilation of a positron-electron pair at rest in the laboratory system, in which two photons are emitted, the relative emission angle is found to be π radians. If the pair has a finite momentum, the photons must carry away this additional momentum and energy, leading to a broadening of the mc^2 gamma line. Thus, the breadth of the line yields information about the state just prior to annihilation.

Green and Stewart[35] used a double coincidence arrangement to measure the angular spread in light metals. From their result it was evident that the photons carried away an amount of momentum which was on the same order of magnitude as the momentum of the conduction electrons. Since it had been shown that the positrons thermalize quickly, it was concluded that they annihilate chiefly with conduction electrons. When heavier metals were used as a target, a two gamma component of higher momentum occurs. In addition, a significant "tail" persists on the plot of coincidences versus angle.[36,37,38] This "tail" was interpreted to result from annihilation with core electrons whose momentum is greater.

In studies with quartz, Page and Heinberg,[39] and co-workers,[40] found that fused quartz had a very narrow angular correlation curve, while crystalline quartz was nearly like the metals. Further studies showed that all materials which possess the long component of lifetime also have a narrow angular distribution curve.

2. Three Gamma Annihilation

Direct measurements of three gamma annihilation were made by de Benedetti and Siegel[41] using a triple coincidence method in which they placed three counters coplanar in coincidence and one not coplanar which was in anticoincidence. Their results are in rough agreement with the theoretical expectation of one triplet annihilation per 370 singlet annihilations.

J. The Temperature Effect in Amorphous Solids

A temperature dependence of the long lifetime component in the annihilation process as well as the variance from material to material

was observed by Bell and Graham.[9] They observed a more or less linear dependence of the long lifetime on temperature between + 20° C and -196° C although no change in the intensity ratio was found within the limits of error. Further investigation[42] on teflon have shown that a curve which plots the long lifetime component, τ_2 versus temperature levels off between liquid nitrogen and liquid helium temperatures. A similar dependence of the three quanta coincidence rate was observed by Graham and Stewart[43] and Wagner and Hereford[44] for several substances. Since the three-quanta annihilation arises from triplet positronium which has escaped pickoff, one is merely observing another manifestation of the temperature dependence of the long lived component. However, in addition to these temperature effects, which are apparently associated with changes in pick off due to thermal expansion, a temperature effect on the angular distribution of annihilation was found by Stewart.[38] A strong enhancement of the narrow component was found in Teflon at 250° C. Although the experimental evidence suggests some identity between the τ_2 and the narrow-component radiation of angular correlation, it is clear that pick off annihilation from the triplet state of positronium with which the long component is associated, should not fall into the narrow component since they involve additional linear momenta. Enhancement of the singlet state by a strong magnetic field also bear out the assumption that self annihilation from the ^1S state is confined to a narrow angular region. It is fairly certain, therefore, that at least the major portion of the narrow component arises from singlet positronium self annihilation and the broad component must be attributed to pick off and direct annihilation.

An interesting effect on the long component occurs when the annihilation medium undergoes a phase change. De Zafra and Joyner[45] studied this effect in water from -240°C to 80°C. As the temperature approaches to melting point the lifetime increases quite gradually and at the melting point it drops substantially then begins to increase with temperature once more, this time at a much faster rate. Wagner and Hereford[44] have shown that the three quanta annihilation for positrons in water, methyl alcohol, and glycerine change markedly at the liquid to solid phase transition and then decreases with temperature in the solid phase.

The variation of τ_2 with temperature is still in need of a satisfactory theoretical explanation. The temperature effect might be related to the order-disorder present in the material. As the temperature is lowered, the order in the solid increases, resulting in an improved orientation of the molecules or atoms. Increased electric fields due to change in molecular orientation might increase the annihilation probability between bound positron and electron of neighboring atoms of molecule.

It has been suggested by Wallace[46] that the temperature effect might be attributed to the creation, at higher temperatures, of larger interstices in the material in which positronium could "hide."

De Zafra and Joyner[45] have interpreted the temperature effect as being actually a density effect, which can be explained in terms of a density dependence on the amount of positronium formed, and therefore on the number of positrons which may decay by the low-momentum process of self-annihilation from the singlet state of positronium.

Stump[47] investigated the influence of pressure on lifetime, subjecting water, Lucite, Teflon, and polyethylene to pressures up to 60,000 lb/in.^{2} No change was observed in water; however, a marked decrease was observed with increasing pressure in Lucite, and especially Teflon and polyethelene, and was found to be roughly proportional to the volume change. Hence, the proposal that the long lifetime variation was mainly the result of variation in density might also explain the temperature effect.

In conclusion, positronium is an atom-like structure in which only electromagnetic forces play a role, there being no nuclear forces present. Despite the short lifetime of this atom (10^{-10} seconds) against annihilation, modern experimental techniques have made possible a detailed study of its properties. It has served as an ideal system in which the calculations of quantum electrodynamics can be compared with experimental results. The latest r-f resonance measurements of the fine structure splitting of the positronium ground state to an accuracy of five significant figures established impressively the exactness of the radiative correction computations to terms of order α^5 .[48]

The second aspect of positron interactions involves positrons in condensed media, solids, and liquids. In this case the primary interest lies in the interactions of the positron with the solid or liquid prior to annihilation, leading to the possibility of bound state formation.

Farrell[49] has pointed out that one of the great virtues of the use of positrons as a tool is that a high energy positron can penetrate into the interior of the sample and then be stopped and become a real member of the electric system. This all happens very fast and from

then on, one needs only consider low energy, nonrelativistic interactions with the surrounding matter. As discussed in more detail later, the annihilation rate and the distribution in the total momentum of the annihilation photon emitted depend in many cases solely on the product of the positron wave function times the wave function of the electron being annihilated. Thus, experimental measurements of the lifetime and momentum distribution give useful information about the interior of a sample. An important advantage of the positron annihilation is that information is transported to the observer in high energy gamma rays which escape without appreciable attenuation or scattering from reasonably small samples; in contrast to, say, soft x-ray emission where surface properties may strongly influence the results.

One drawback of the positronium annihilation method is that the tool used for measuring the system changes the system, i.e., the presence of the positron distorts the electronic wave function an appreciable amount.

The purpose of this experiment has been to measure the long lifetime component in various solids at different temperatures and to determine this variation with temperature. It is hoped that a knowledge of this temperature parameter--or the density parameter which may be obtained from the temperature--through its effect on the positronium τ_2, will soon enable positron annihilation to become a solid state research tool.

CHAPTER II

THEORY

A. Annihilation Properties

If an electron makes a transition to a vacancy in the negative energy levels, which has been identified as the positron, the energy may be released in a number of ways. The most common of these--and the only one energetically permissible using a Na^{22} source--is by the emission of photons. If the energy were great enough, however, a meson pair or a nucleon and an anti-nucleon could be created.

There are essentially three different types of pair annihilation: (1) annihilation of a free positron with a free negatron in relative motion towards each other; (2) annihilation of a bound system of positron and electron; and (3) annihilation in the presence of a coulomb field or nucleus. The latter alternative is the only process that does not exclude one-photon annihilation. In this case the target atom receives the excess momentum.

1. Two-Quanta Annihilation

The lowest order process for the annihilation of a free pair is the emission of two photons. The relativistic cross section for this process was derived by Dirac,[1] and his results are discussed by Heitler[22] and Jauch and Rohrlich.[50] Detailed calculation in the plane wave approximation gives the result

$$\sigma_{2\gamma} = \frac{\pi r_0^2}{\gamma+1}\left[\frac{\gamma^2+4\gamma+1}{\gamma^2-1}\right]\ln\left(\gamma\sqrt{\gamma^2-1}\right) - \frac{\gamma-3}{\gamma^2-1} \qquad (1)$$

$$r_0 = e^2/mc^2$$

r_0 = classical electron radius

$\gamma = \frac{E_+}{4\pi\varepsilon_0 c^2}$, E_+ being the energy of the positron

e = electron charge

ε_0 = dielectric constant in vacuum

m_0 = electron mass

c = velocity of light

When the positron is nonrelativistic as in our case, (1) reduces to

$$\sigma_{2\gamma} \simeq \frac{\pi r_0^2 c}{v_+}, \qquad v_+ = \text{positron velocity} \qquad (2)$$

However, since v_+ is Lorentz-invariant, (2) holds when v_+ is the relative positron-electron velocity. The probability for annihilation of a positron per unit time or the rate of annihilation is, from equation (2)

$$R_{2\gamma} = \sigma n_- v = \pi r_0^2 n_- c$$

or $R_{2\gamma} = 7.50 \times 10^{-15}\, n \ (\text{sec}^{-1})$

and $$R_{2\gamma} = 4.52 \times 10^{9}\, \frac{\rho Z}{A} \qquad (3)$$

where n_- is the electron density of the medium so that ρ, Z and A are the density, atomic number, and atomic weight respectively of the medium. The mean life of a positron of nonrelativistic velocity is then given by $1/R_{2\gamma}$. More properly, n_- in (3) should be replaced by the density of electrons considering their proper spin orientation at the position of the positron. In terms of an electron wave function ψ_s

(subscript S refers to singlet spin orientation) one obtains, setting $\lambda_c = \frac{\hbar}{mc}$ and $\alpha = \frac{e^2}{\hbar c}$

$$R_{2\gamma} = 4\pi \lambda_c (\alpha^2 mc^2/\hbar) \psi_S(0) \tag{3'}$$

Equation (3') might be interpreted by considering the electrons as spheres of radius λ_c which, when they overlap, annihilate at the characteristic rate.[60] The factor 4 appears because only one collision in four forms a singlet state. However, equations (1) to (3) cannot be verified directly since the positron causes a serious deformation of the electron configuration of the medium before annihilation. Thus, strictly speaking, n_- cannot be calculated from the macroscopic properties. Equation (3') has been solved by Pirenne.[4] His result for the singlet lifetime was $\tau_2 = 1.25 \times 10^{-10}$ seconds.

2. Three-Quantum Annihilation

When the annihilation via two quanta is ruled out by the symmetry of positron-electron wave function, three gamma annihilation is the lowest order possible. This is true specifically in ^3S states which make up 3/4 of all collisions at thermal energies. Ore and Powell[6] have calculated the ratio of the three-quantum to two-quantum rate and find

$$\frac{\tau_2}{\tau_3} = \frac{4}{9\pi}(\pi^2 - 9)\alpha \simeq \frac{1}{1115} \approx \frac{\alpha}{8} \tag{4}$$

or numerically

$$\tau_3 = 1.4 \times 10^{-7} n^{-1} \text{ (sec)} \tag{5}$$

For the ratio of the spin averaged cross sections

$$\frac{\sigma_3}{\sigma_2} = \frac{3/4\ {}^3\sigma_{3\gamma}}{1/4\ {}^1\sigma_{2\gamma}} = 3\left(\frac{{}^1\tau_{2\gamma}}{{}^3\tau_{3\gamma}}\right) \tag{6}$$

or

$$\sigma_{3\gamma} = \frac{4}{3}(\pi^2 - 9)\alpha r_0^2 c/v \tag{7}$$

These results imply that a ^1S state annihilates 1115 times faster than the corresponding ^3S state, and the ratio of the numbers of three-quantum to two-quantum events in collisions with statistically oriented spins is 1/372. From Pirenne's results for τ_1, we have that τ_2 should be 1120 longer, or $\tau_2 = 1.4 \times 10^{-7}$ seconds.

B. Selection Rules

The selection rules for two and three photon annihilation may be deduced in a nonrigorous fashion by considering only the conservation laws. Consider first the case of ^1S positronium with little or no momentum. Upon annihilation, an energy of $2mc^2$ must be released with no net momentum in the center-of-mass coordinate system. Because the annihilation takes place from the singlet state of zero total angular momentum, there can be no angular momentum in the electromagnetic field. If one photon is plane polarized in the vertical direction, the other must be plane polarized horizontally. Two-quantum annihilation is, however, completely forbidden for all states with $J = 1$, e.g., for ^3S state. Since each of the two quanta has an intrinsic angular momentum of $\pm\hbar$ along its direction of propagation, which we

arbitrarily call the z-axis, the two photons can only form states with z-components of angular momentum $m=0$ or $m=2$. The latter are clearly ruled out for a total angular momentum $J = 1$. The two-quantum state with $m=0$, representing for example two right hand circularly polarized quanta, is left unchanged when the coordinate system is rotated around the x-axis to change $+z$ to $-z$. However, the sign of the wave function of any state with $J = 1$ and $m=0$ changes under rotation. This possibility is thus excluded as it is violation of the symmetry properties of the system.

The same results are obtained employing the formalism of the space inversion operator Π, the charge conjugation operator Γ, and the space inversion operator $\sum$ by Jauch and Rohrlich.[50]

Restating our selection rules for the general case we have that positronium states of even charge parity, i.e., the singlet states of even L (total orbital angular momentum quantum number) and the triplet states of odd L decay only into an even number of photons, of which the two-photon decay is of primary importance. On the other hand, positronium annihilation into an odd number of photons (of which three is the minimum) can take place only from an odd parity state, i.e., a singlet state of odd L or a triplet state of even L.

C. Formation of Positronium

1. Ore Gap Theory

As discussed in the introduction, it is generally accepted that the long component of the lifetime is due to the formation of positronium, which is probably best regarded as a natural and common fate of a positron being slowed down. In metals, however, the conduction

electrons are free to interfere with any positronium atom which might be formed, and can either strongly modify the positronium or prevent its independent existence altogether. In insulators, positronium formation seems to be a normal occurence. The ionic crystals evidently comprise a special class in which the formation of a positronium atom, stable with respect to subsequent dislocation, is energetically not permitted. The energetics of positronium formation in gases was first discussed by Ore[51] and has been reviewed by Deutsch.[52] With slight modification, Ore's theory can be adapted to solids.[49,53,54] The binding energy of positronium, W_{pos}, is one-half a rydberg or 6.8ev in free space; it is slightly less in an insulating solid, and considerably less in a metal. Let us designate the ionization potential of a molecule of the material by I. This is on the order of 10 ev for most dielectric solids, 12.5 ev in water, 9.2 ev in benzene.[54] Energy balance then requires $E > I - W_{pos}$ where E is the kinetic energy of the positron. As long as E is greater than the lowest electronic excitation energy of the molecule (V_1) this excitation, along with inelastic scattering of the positron, will compete with positronium formation. At energies above the ionization energy, inelastic scattering with ionization will compete and will generally have a larger cross section because of the greater density of final states associated with the presence of two free particles in the final configuration. The limited range of energies in which positronium can form is called the "Ore gap."

In Figure 2(a) is shown an "Ore diagram" for an ionic crystal, where for the moment, the coulomb interaction energy between the positron and the ions is not taken into account.

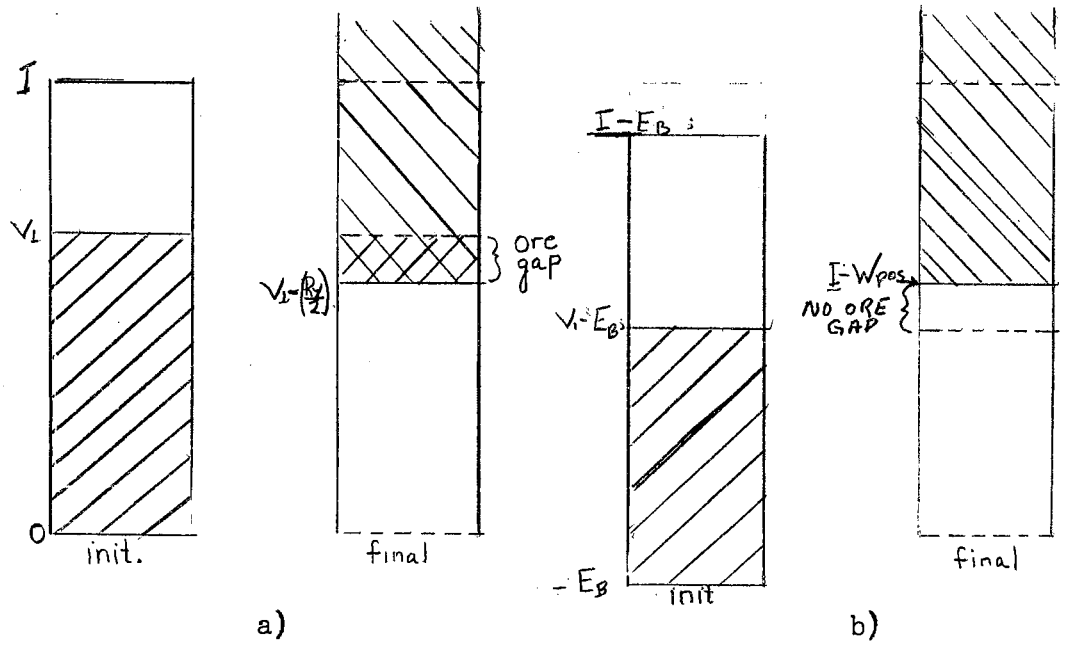

Figure 2. The Ore diagram for (a) no energy shift (b) energy shift. The energy shift destroys the Ore gap and prevents positronium formation. (After Ferrell)

The left hand side shows the possible initial states of the system and is shaded below V_1; in this case the lowest excitation energy level is the bottom of the conduction band. The area above the V_1 is not shaded as we neglect positronium formation due to the much more likely interactions of inelastic scattering and electron excitation. The possible final states available to the system after capture of an electron by the positron are shown by the right hand portion of Figure 2(a). Because of the requirement of energy conservation, the capture process can only take place if the two regions overlap, forming the "Ore gap." The condition that there be an Ore gap is simply $V_1 > I - W_{pos}$.

In ionic crystals, the bottom of the conduction band lies below the ionization potential, making positronium formation unfavorable. This general feature is a result of the ordering of the ions in a

regular lattice and disappears when sufficient disorder is introduced, as in the polymers, fused materials, and organic waxes. The ionic crystals are also quite different in this respect from the molecular crystals, where there is no electron energy band not already filled which is significantly below the ionization potential.

Looking again at the ionic crystal picture considering the Coulomb interaction, we have another force working against positronium formation. This is illustrated in Figure 2(b) and is associated with the lowest non-positronium state of the positron in the system. Let V_{ap} be the positron affinity, i.e., the energy required to take a positron out of this state and remove it from the crystal. In this case if positrons of energy greater than $(V_1 - V_{ap})$ capture electrons, the resulting positronium atoms break up again. The effect of binding of positronium to the crystal is not shown in Figure 2(b) but must be considered. Thus, the criterion for the Ore gap must, therefore, be modified to read $V_1 - V_{ap} > I - W_{pos} - E_p$ or $(I - V_1) + V_{ap} - E_p < W_{pos}$

where E_p is the binding energy of positronium atoms to the crystal. By analogy with general usage, by which the quantity $(I - V_1)$ is called the "electron affinity," Ferrell calls V_{ap} and E_p the "positron affinity" and the "positronium affinity" of the crystal, respectively.

The condition for positronium formation (or more properly, that an Ore gap exist) is now that the sum of the electron and positron affinities minus the positronium affinity shall be less than the positronium binding energy. Thus, it is pointed out that the affinity of the crystal for positrons works equally as effectively as the affinity for electrons against positronium, while the affinity of the crystal

for positronium works in favor of positronium formation.

Another factor affecting the creation of positronium is the presence of possible modes of collision which quickly moderate the positron through the Ore gap. Such a mechanism is the excitation of the vibrational states of the molecule. The availability of vibrational modes of fairly high frequency will work against positronium formation.

In the case of metals, an Ore gap does not exist because of the large number of conduction electrons which lower the binding energy very considerably below 6.8 ev.

D. Triplet to Singlet Conversion

In this section we will deal with the lifetime distribution of those positrons which (1) do not annihilate in flight, but get through the Ore gap without having captured an electron, and (2) the positrons which do form positronium. In case (1), we may assume that the positron will have a greater potential energy inside the molecule than out because of its ability to attract electrons. Wallace[53] considers each molecule as a Fermi gas of molecular dimensions. Hence, such a positron can be expected to contribute to the short lifetime. It may be captured to form a bound state in some cases; in this event again it should contribute to the short lifetime. In case (2) the positronium will decay with $\tau_1 = 1.2 \times 10^{-10}$ seconds if it is singlet. If it is triplet, it need not decay with the theoretical value of $\tau_2 = 1.4 \times 10^{-7}$ seconds. The positronium atom will be scattered continually by the molecules of the material. In this scattering process, three mechanisms have been proposed which will convert orthopositronium to parapositronium thereby shortening its natural triplet

lifetime. The first possible explanation was that the electron underwent a spin flip on collision. Ore[51] pointed out, however, that spin flip through magnetic interaction would take on the order of 10^{-5} seconds, whereas the radiative transition has a macroscopic lifetime. A second explanation was proposed by Dixon and Trainor[55] who noticed that the long component of the lifetime was about eight times the short component. The 2s state of parapositronium happens to also have a lifetime eight times that of the 1s state. This coincidence suggested that the excited state of positronium was responsible for the τ_2 and not ortho-para conversion. Almost immediately, however, Wallace[46] pointed out that this hypothesis is untenable on various grounds. In the first place, the metastability is associated with a symmetry selection rule, based on the fact that the 1s and 2s states, being spherically symmetrical, do not combine in the presence of the electromagnetic field. However, the "2s" if it existed in a solid, would have its spherical symmetry perturbed considerably by the crystal potential, and so could be ecpected to decay quite rapidly. Wallace further pointed out that certain experimental facts are inconsistent with the hypothesis: (a) the nonexistence of a very long lifetime associated with formation of triplet positronium, (b) the evidence from magnetic quenching experiments for the association of the τ_2 lifetime with triplet positronium, in analogy with the situation in gases,[7,8] (c) Furthermore, Brock and Streib[56] performed an experiment which was designed to detect the Lyman-α line associated with decay of excited positronium diffusing out of a gold surface, with negative results. Ferrell in addition, claims that the Ore gap is always much smaller for the excited states than for the ground state, as the ground-state binding energy of

ry/2 must be replaced in inequality (1) by W_{Ps} = ry/8 in dealing with energetics of 2s formation. Thus, even if the inequality is satisfied for the 1s state it may very well not be satisfied for the 2s state.

Bell and Graham tried to account for their unexpected value of in terms of an exchange collision, in which the positron would exchange an electron of opposite spin for one of parallel spin during a collision. Wallace[53] and Ferrell[49] point out that this mechanism is also objectionable as there is no reason to expect such a conversion in the insulators exhibiting the τ_2 component. These materials all consist of atoms with closed shells in which the electron spins are paired off, therefore the exchange process could take place only through excitation, and this will be impossible energetically in slow collisions.

The remaining possibility was suggested by Garwin[17] as an alternate to the exchange collision. He hypothesized that the positron might annihilate with an electron of appropriate spin from a neighboring atom. The "pickoff" annihilation mechanism is the currently accepted theory explaining why the long component is significantly less than 10^{-7} in amorphous solids.

E. Factors Effecting the Conversion Rate

After Wallace[53] and deZafra and Joyner[45] pointed out the correlation between the density and the τ_2 component, it remained until recently a puzzle why the τ_2 increased with temperature. The τ_2 is determined by the rate of "pickoff" and the common situation is for reaction rates to increase with temperature. Brandt, Berko and Walker[57] applied quantum mechanics for the special case of a polytetrafluoroethylene (Teflon) sample with good results. They chose this particular sample

because it would conform reasonably well to the following model.

(1) The mutual positronium and lattice polarization can be neglected.

(2) The lattice constituents are approximated by square potentials of height V_o, electron density ρ_o, and radius r_o, or correspondingly, the "excluded volume" v_o, each centered in a cell volume v_1 of radius r_1.

(3) The positronium atoms are thermalized and can be treated in the zero-velocity $(\vec{k}_{pos} \simeq 0)$ approximation.

In the nonrelativistic approximation, the spin average of the 2γ and 3γ annihilation rates, γ_2 and γ_3 of an electron-positron pair in the para and ortho orientation, respectively is given by

$$\gamma_2 = \pi r_o^2 c \left|\Psi(r_+)\right|^2 \tag{1}$$

$$\gamma_3 = \gamma_2/373 \tag{2}$$

In a lattice L of electron density distribution $\left|\Psi_L(r)\right|^2$ composed of neutral atoms or molecules with closed shells, i.e., in the absence of paramagnetic impurities, the electron pickup rate γ_p of orthopositronium in L is

$$\gamma_p = \pi r_o^2 c \int \Psi_L^*(\vec{r})\, \Psi_{b+}^*(\vec{r})\, \Psi_{b+}(\vec{r})\, \Psi_L(r)\, d^3r \tag{3}$$

where Ψ_{b+} is the wave function in the field of the electron to which it is bound as orthopositronium and the field of the lattice.

The problem is to evaluate equation (3) as a function of the properties of L .

To evaluate equation (3), we set $$\psi_{b+} = \alpha(r_{b+})\,\psi_{pos}(\vec{r}_o) \qquad (4)$$

where α is a polarization function and the subscript O refers to the positronium center of mass. However, the Brandt model assumes $\alpha = 1$, so (3) becomes

$$\psi_p = \pi r_o^2 c \rho_o \int \psi_{pos}^{*} \; \psi_{pos} \; d^3r \qquad (5)$$

Equation (5) is then solved by means of the Wigner-Seitz approximation, assuming a unit cell of volume v_1 in which v_o is centered.

Their solution for equation (3) is

$$\gamma_p = \frac{\pi \rho_o c r_o^2}{1 + F(U_o, \rho_o, \gamma)} \qquad (6)$$

where F is a function of the particular geometry of the model chosen. Temperature does not appear explicitly in (6), because F is calculated in the $(\vec{k}_{pos}=0)$ approximation and the lattice is assumed to be adiabatically rigid. The authors gave explicit functional solutions for F with three geometrical models--layer lattices, hard sphere lattices, and the cylinder geometry of chain lattices. For the chain lattice model of polytetrafluorethylene, they obtained very good agreement with the experimental observations of Bell and Graham,[9] Berko and Landes,[63] plus data of their own.

CHAPTER III

EXPERIMENTAL METHODS

The classification of equipment used for measuring time intervals in the 10^{-6} to 10^{-10} second range falls in two categories, "delayed coincidence circuits" and "time sorters." The delayed coincidence circuit is a single channel device in which voltage pulses are counted when they are in coincidence. The time sorter circuit is a multichannel time measuring device which converts a time interval between two pulses to a single voltage pulse. These voltage pulses are then sorted into channels according to pulse height by a multichannel analyzer. Both of these types of circuits were employed in this work, the former circuit being used to check the detector and take preliminary data while the latter was used for the rapid accumulation of data.

The operating principles of the time sorter circuitry are as follows:

(1) The detectors produce electronic pulses whose amplitude corresponds to the energy of the gamma incident upon the fluors. Thus the 1.28 Mev "creation" gamma are roughly $2\frac{1}{2}$ times the size of the 0.51 annihilation pulse. Traces of photographs of these pulses are illustrated in Figure 3(a).

(2) For each of these pulses, the detector gives two outputs. One of these outputs is called the energy or side channel output. The

other is the time pulse which is transmitted to the "fast circuitry." A discriminator in the side channels blocks all pulses which are not the desired size. Any pulse whose amplitude is insufficient to correspond to a 0.51 Mev gamma is not passed in the 0.51 channel. Similarly, the 1.28 Mev side channel accepts only those signals correspondingly large enough to represent "creation" quanta.

(3) After amplification, the time pulses which have sufficient energy produce a step voltage (rise time estimated at less than one millimicrosecond) with a flat plateau of about five microseconds. These pulses are represented in Figure 3(b).

(4) Upon reaching the time-to-amplitude converter, these steps are clipped to a fixed length, τ_o, (about 15 millimicroseconds) by a set of identical shorting stubs. These pulses are illustrated in Figure 3(c).

(5) If a pulse is produced by the second limiter within a time τ_o of activation of the first limiter, a superposition of the two wave forms occurs at the input to the time-to-amplitude converter. If the converter is biased to the level shown in Figure 3(d), only the overlap portion of the pulse will be transmitted to the bias of the integrating circuit.

(6) In the time-to-amplitude converter, a fast switching transistor is operated by the overlap pulse, and a fixed current is integrated for a period of time determined by the length of overlap. After amplification, a pulse of the form sketched in Figure 3(e) is obtained.

(7) A gate circuit on the multichannel analyser is operated by coincidence pulses in the side channels discussed in step 2. When the coincidence requirements are satisfied, the multichannel analyser will

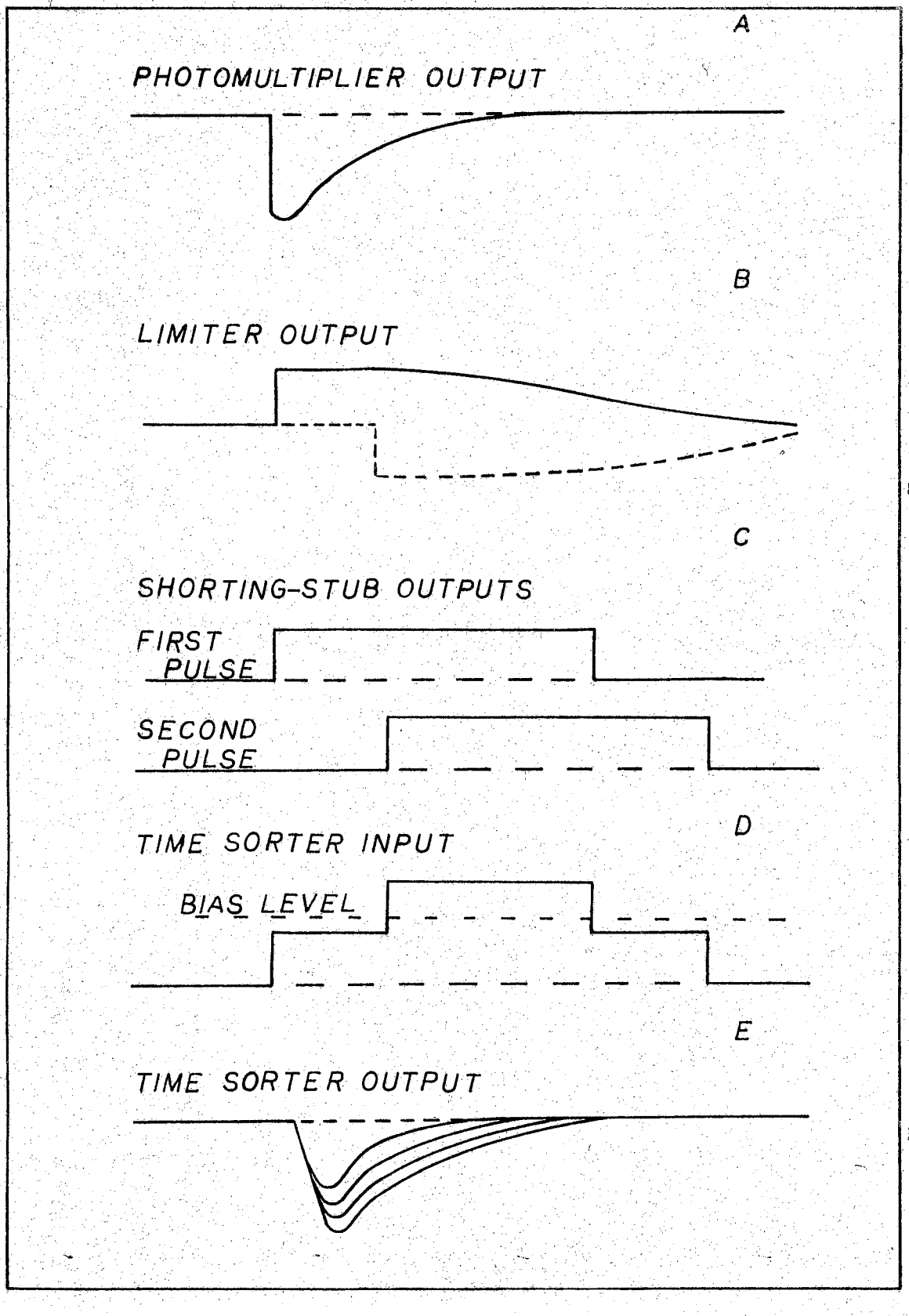

Figure 3. Electronic Pulse Forms.

accept an amplitude pulse from the converter.

The time difference between the time of appearance of the 1.28 Mev and the 0.51 Mev quanta is, then, readily obtained from the conversion factor of time increment per channel of the converter-analyser system.

A complete block diagram of the system is shown in Figure 4.

A. Detectors

The detectors used in both circuits consisted of an RCA 6342-A photomultiplier tube, an NE-102 scintillator, and a cathode follower. As mentioned, two outputs are taken from the detector. The time pulse is taken from the anode and the energy pulse is taken from the eighth dynode of the photomultiplier.

The mean time delay for the appearance of the first photoelectron from the photocathode of a scintillation counter as given by Post and Schiff,[58] is $\bar{t} = \tau/R(1+\frac{1}{R})$ where τ is the mean life in the scintillation in the phosphor, and R is the total number of photoelectrons produced during the pulse. Since R is proportional to the light output from the fluor, it is strongly dependent on the optical coupling of the crystal and the efficiency of the light pipe, etc. For the best resolution $\bar{t}$ should be minimized. However, the expression for $\bar{t}$ considers only that portion of the scintillation counter consisting of the crystal and photocathode, it is not the overall detector resolution unless the spread in transit time of the phototube is negligible in comparison to $\bar{t}$ and if the photomultiplier is capable of sufficient gain for the detection of single electron pulses from the photocathode.

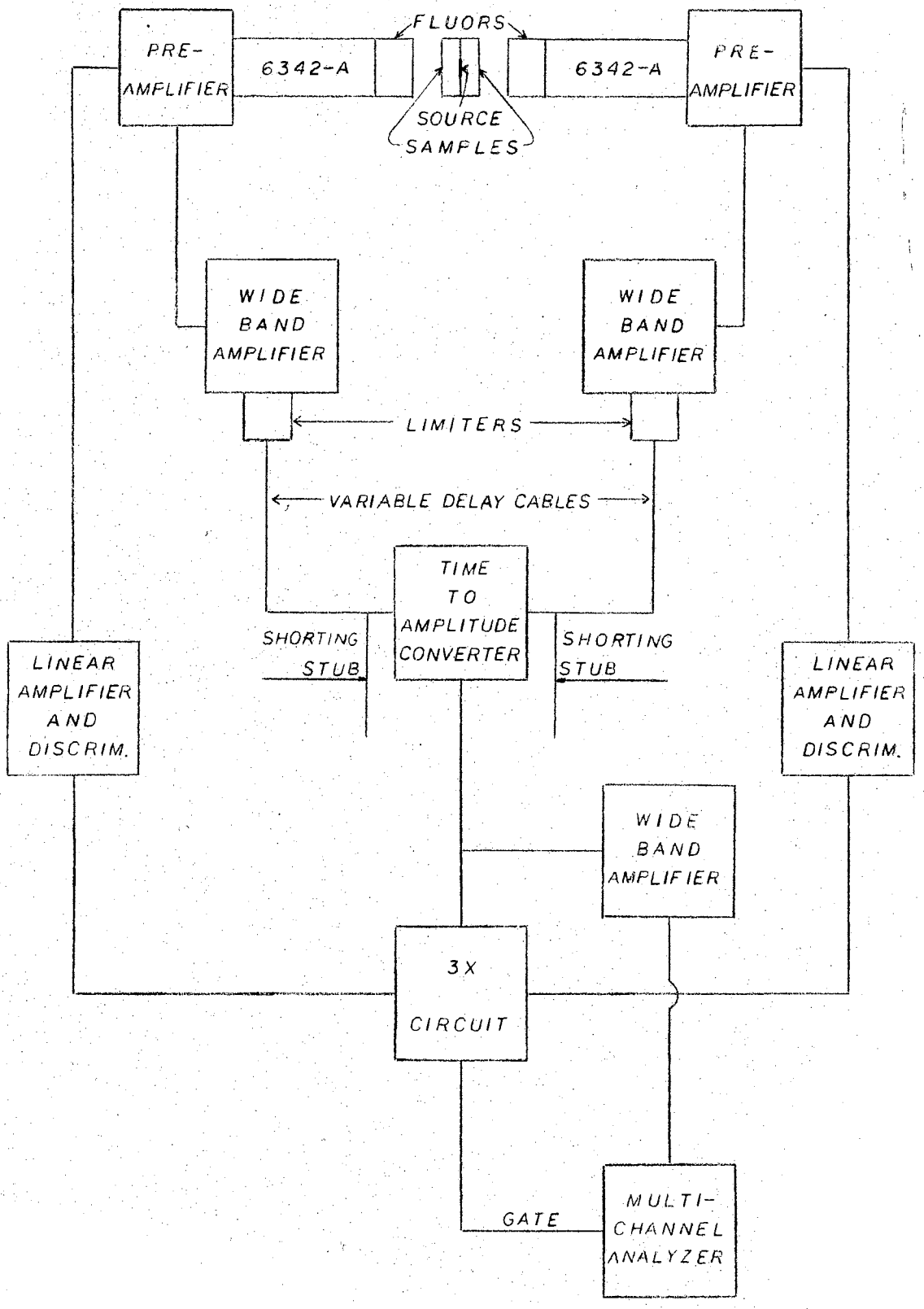

Figure 4. Complete Block Diagram of Electronic System.

1. Photomultipliers

To meet the requirements of transit time and gain that are required, the RCA 6342-A was selected. This tube is constructed with an end window photocathode, which is curved in order to obtain better spherical geometry. This assures good electron collection by the first dynode from all regions of the semitransparent cathode surface. The maximum value of the transit time in this multiplier tube is four millimicroseconds. The current gain of the 6342-A at the voltage operated at during our work is on the order of 8×10^5. Other advantages offered by the 6342-A are two focusing electrodes--one of these shapes the field which directs photoelectrons from the photocathode to the first dynode; the other permits optimizing the magnitude, uniformity or speed of the pulse.

The spectral response of the multiplier tube is S-11, peaking around 4400 Angstroms.

Magnetic shielding was provided for the tube by a cylindrical shield of Mu metal, which fit snugly around the glass case of the tube and was held at cathode potential.

The gain and stability of the tube were maximized using standard aging techniques for a period of six months under dark conditions. The tube was then operated successfully at 1700 volts, somewhat higher than recommended by RCA. It was felt the gain characteristic of the tube was more suited to our purpose at this operating potential.

When it became necessary to remove the high voltage from the phototube, extreme caution was exercised in returning the supply voltage to operating value over a long enough period of time to preserve stability of the dynode-bleeder string combination. The NE 160 was

permanently coupled to the light pipe by a resin cement. Good optical coupling between the pipe and photomultiplier was obtained with Dow Corning QC-2-0057 silicone grease. (Dow Corning Corporation, Midland, Michigan.)

2. Limiters

A good limiter must produce flat top pulses with short rise times and constant amplitudes. The primary circuit element for the control of these parameters is the tube. The most commonly used tubes in these applications are the 404-A and the E 180 F.

A circuit designed by Bell et al.,[59] and reviewed by Lewis and Wells,[60] proved to be satisfactory in our application. The requirements on the pulses for this circuit are negative input pulses having fast rising edges, followed by a slow exponential decay to zero. The schematic diagram of the circuit is shown in Figure 6.

3. Scintillators

The scintillation phosphors used to convert the gamma ray energy to visible light were the NE102 and the NE160. The NE102 was used for measurements at room temperature and below, while the latter was used for the high temperature studies. These crystals, manufactured by Nuclear Enterprises, Winnipeg, Canada, both have a pulse height 60% relative to that of anthracene, and have their maximum emission peak at 4200 Angstroms. The NE102 decay constant is 3.5×10^{-9} seconds, and while this datum had not yet been determined by Nuclear Enterprises for the high temperature phosphor, the manufactures said that it was in the millimicrosecond region.

NE160 Plastic Phosphor is stable at temperatures up to 150°C but after some time at this temperature the light output falls. After 12

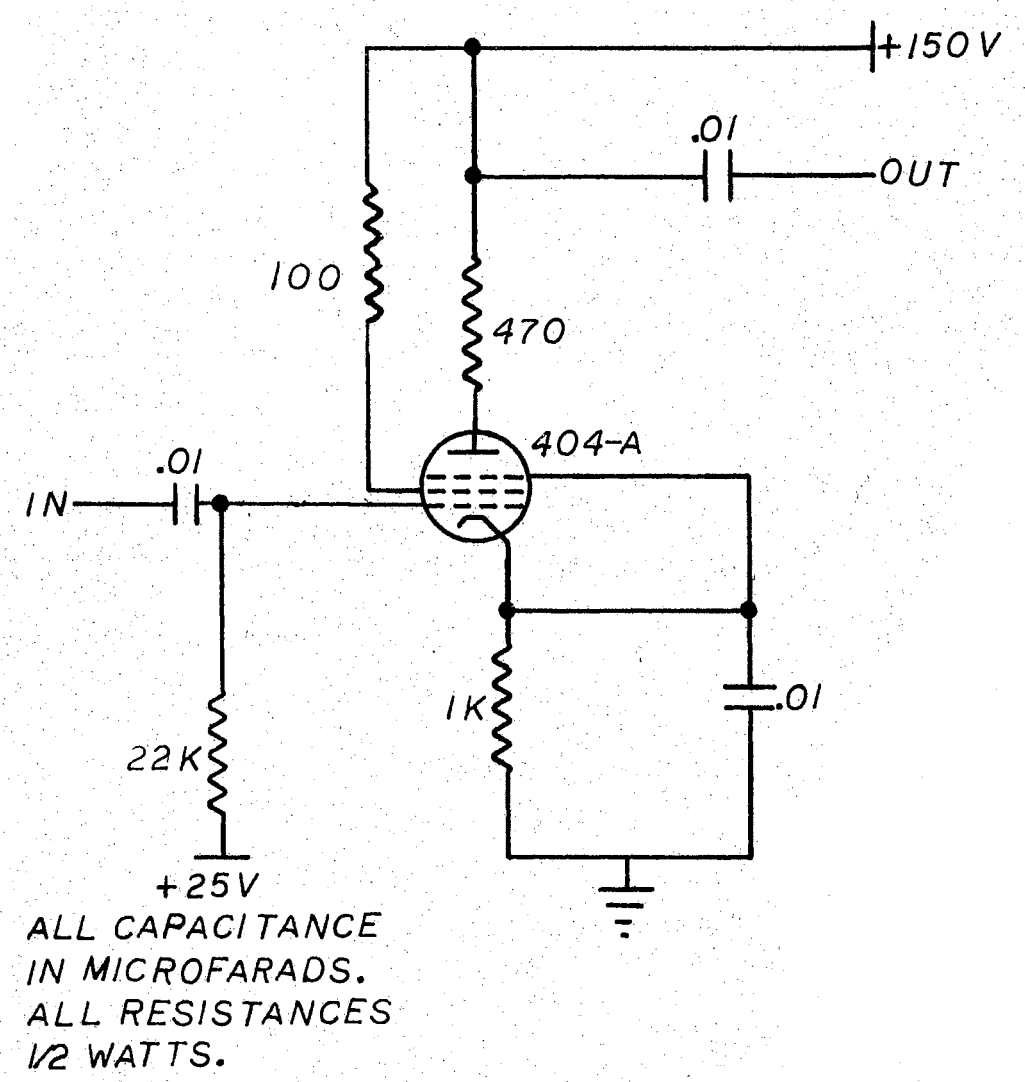

Figure 5. Schematic Diagram of Limiter.

hours at this temperature the relative pulse height is 47% and after 36 hours is 36%. However, no readings were taken which subjected the fluors to a high temperature for longer than 8 hours.

In order to keep the temperature of the photomultiplier constant at room temperature, the light was piped from the NE160 fluor to the end window photomultiplier by means of a Nuclear Enterprise polyvinyl-toluene light pipe, six inches long.

B. Shorting Stubs

The shorting stubs consisted of two identical (183 cm) lengths of RG-8/u which has a characteristic impedance of 50 ohms, the value required for matching the impedances between the stub and the two, effectively parallel, 100 ohm (RG-7/u) cables to the limiters. Thus, the shorting stub is terminated in its characteristic impedance, preventing multiple reflections. A reflection does occur, however, in the limiter cable, the terminating impedance of these cables being the parallel combination of the shorting stub and the other cable: $\frac{50 \times 100}{50 + 100} = 33\%$. Consequently, a reflection of an amount $\frac{100 - 33}{100 + 33} = 50\%$ occurs when the limiter output pulse strikes this junction. However, our input pulse to the time-to-amplitude converter is still 0.5 volts, quite sufficient to operate the transistors.

C. Time-to-Pulse Height Converter

The requirements for the time-to-pulse height converter are good resolution, linearity of response in the millimicrosecond range, and

high electronic stability. Two such circuits have been developed, one developed by Jones[61] employing the microwave diodes which act as fast current switches followed by a Miller integrator. The other circuit was developed at Columbia by Simms[62] and consists of two fast switching transistors followed by a third integrating transistor. Both circuits satisfy our requirements equally as well, so the simple circuit of Simms was chosen.

A simplified diagram of the converter is given in Figure 6. In the quiesent state, the two transistors T_1 and T_2 in the input circuit are both conducting, and the output transistor T_3 is cut off. When either of the input transistors is cut off by a positive pulse, all of the current flowing through R_2 is carried by the other input transistor. The purpose of R_2 is merely to act as a constant current source. The value of this resistor in our circuit was 15K ohms. When coincidence occurs, T_1 and T_2 are both cut off, and the current is switched into T_3, where it is integrated at the collector of this transistor. The amplitude of the voltage pulse is given by $V = I \cdot \Delta t/C_s$, where C_s is the stray capacitance associated with the physical layout of the circuit and Δt is the time of pulse overlap. We see that for maximum amplitude, as well as a more desirable pulse shape, C_s should be a minimum.

All of the biasing networks are shown in Figure 7 which is the complete schematic drawing. Simms recommends that Western Electric 2N1195 transistors be used for short overlap times. He found it necessary to include a 100 ohm resistor in the base of T_3 to decrease the switching time and decrease the single to doubles ratio, as the bias required to reject singles pulses was so large that the transistor would not switch

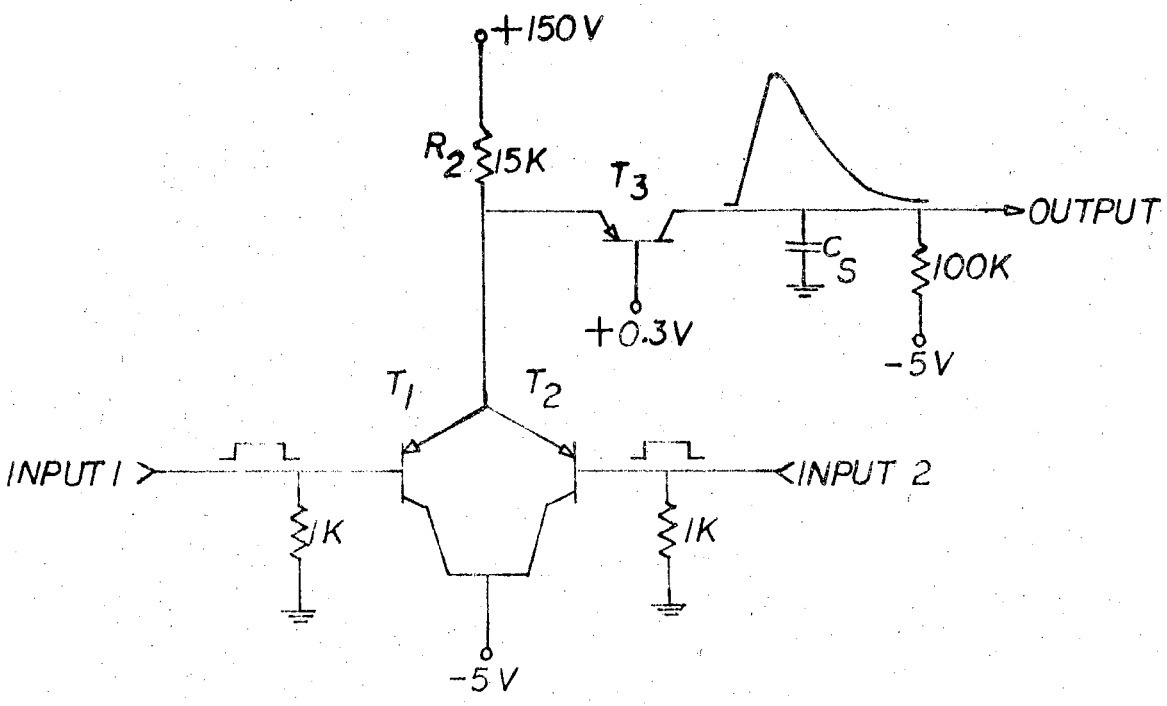

Figure 6. Simplified Time-to-Amplitude Converter Schematic Diagram.

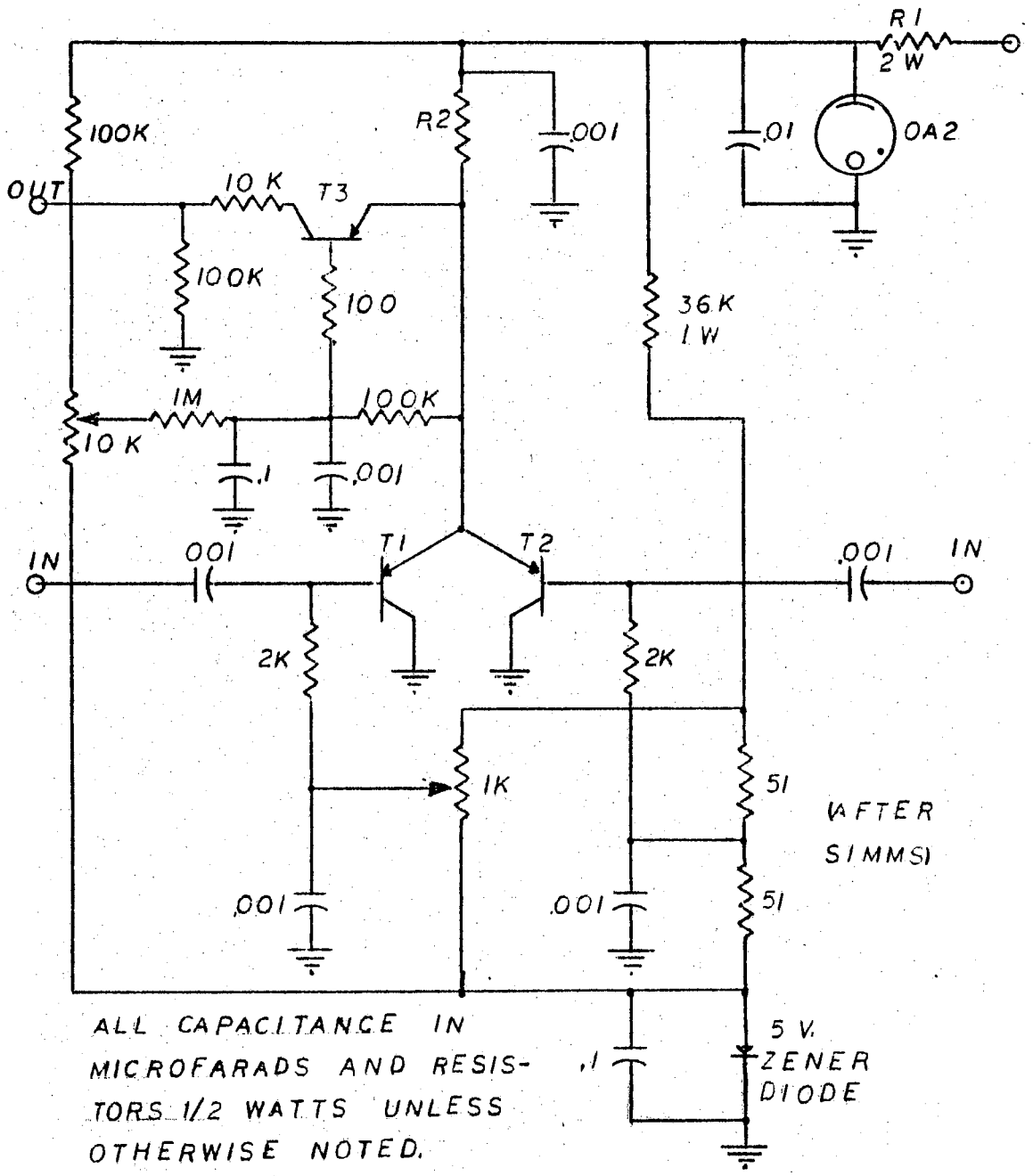

Figure 7. Complete Time-to-Amplitude Converter Schematic Diagram.

as quickly as was necessary. The Philco 2N501 was also tried in this connection with no appreciable difference resulting.

T_1 and T_2 were chosen to be the two transistors whose parameters were the most nearly alike as determined by a transistor checker. To obtain optimum operational balance, the 10K pot is lowered until single pulses are observable at the output. The 1 K pot is then adjusted so that the output pulses have the same amplitude with either input removed. After this balance has been achieved, the 10 K variable resistance is increased to cut out the single pulses.

The purpose of R_1 is to allow this instrument to be used on the overall system power supply. However, for our circuit, we had available a Heathkit power supply which we used solely to power the converter. Thus, R_1 was unnecessary.

D. Associated Equipment

(1) A C Line Voltage Regulator

The A C line voltage regulator which supplied all power to the apparatus was the Sorensen Model #20008 (Sorensen & Company, Inc., Richards Avenue, South Norwalk, Conn.). The regulation accuracy is plus or minus 0.1% against line or load at the normal input frequency with a resistive load.

(2) Photomultiplier Power Supplies

The photomultipliers were powered with Hamner Model N-401 regulated high voltage power supplies (Hamner Electronics Co., Inc., Princeton, New Jersey). These power supplies have a regulation of 2.5 parts per million per milliampere through the range of 0-5 milliamperes. Their stability against line voltage changes is three parts per million

per volt in the range 105-125 volts. The ripple is rated at less than three parts per million peak to peak.

(3) Pulse Amplifiers

The pulse amplifiers used were Hewlett-Packard 460AR wide band amplifier (Hewlett-Packard Company, 275 Page Mill Road, Palo Alto, California). The most important feature in choosing the pulse amplifier is a millimicrosecond rise time. The Hewlett-Packard has a rise time of about three millimicroseconds with no appreciable overshoot.

(4) Coincidence Circuit Amplifier and Discriminator

Since the coincidence circuit is part of "slow circuitry" the fast rise time is not the important factor in choosing this amplifier. Rather we are interested in a higher gain and a pulse height analysis. For this reason, the Baird Atomic Model 215 nonoverloading linear amplifier was selected (Baird Atomic, 33 University Road, Cambridge 38, Mass.). The specifications of this instrument are rise time, 0.2 microseconds; maximum gain 90 to 6,400 by choice of coarse and fine gain controls; decay time, 1 microsecond; discriminator linearity, 0.2%.

(5) Triple Coincidence Circuit

The triple coincidence circuit used was a locally made coincidence-anticoincidence analyser patterned after the Advance Radiation Engineering Corporation (P. O. Box 918, Garland, Texas) Model 401. This instrument has a resolving time of 0.5 to 20.0 microseconds continuously variable through adjustment of individual channel gates. The output pulse is a positive or negative five microsecond rectangular with the amplitude adjustable from zero to 25 volts.

(6) Multichannel Analyzer

The multichannel analyzer employed was the 512 channel Nuclear Data

Model ND130 (Nuclear Data, Inc.,

Data were collected in 128 channels of the analyzer. The pulses were read into the detector input mode and the internal amplifier gain was set at 1.0. The output of the triple coincidence circuit was cabled to coincidence input.

Having accumulated, the data were inspected on a Techtronix 503 oscilloscope and read out on an IBM typewriter. Typical settings for the analyzer were coarse energy gain, 1; fine energy gain, 0; energy zero, 1.5.

The amplifiers, power supplies, and limiters are shown in Figure 8(a). The time-to-amplitude converter, multichannel analyzer, and display oscilloscope are shown in Figure 8(b). The detector assembly is illustrated in Figure 9. The source is in the mylar sandwich within the aluminum ring between the detectors.

E. Calibration of the Time-to-Amplitude Converter

Two methods are commonly used for the calibration of time-to-amplitude converters. The first consists of placing a source of coincident gamma rays between the counters and measuring the pulse amplitude as the shorting stub length is varied. When the shorting stubs are lengthened, the overlap time is increased by twice the electrical length of the increase in cable length. Since the pulse height is proportional to the overlap time, the change of cable length--hence the time in millimicroseconds--can be plotted vs. channel number.

The other method consists of changing the time delay in one channel. The latter method was employed in this work in the following manner. The cable length between the limiter and the time-to-amplitude

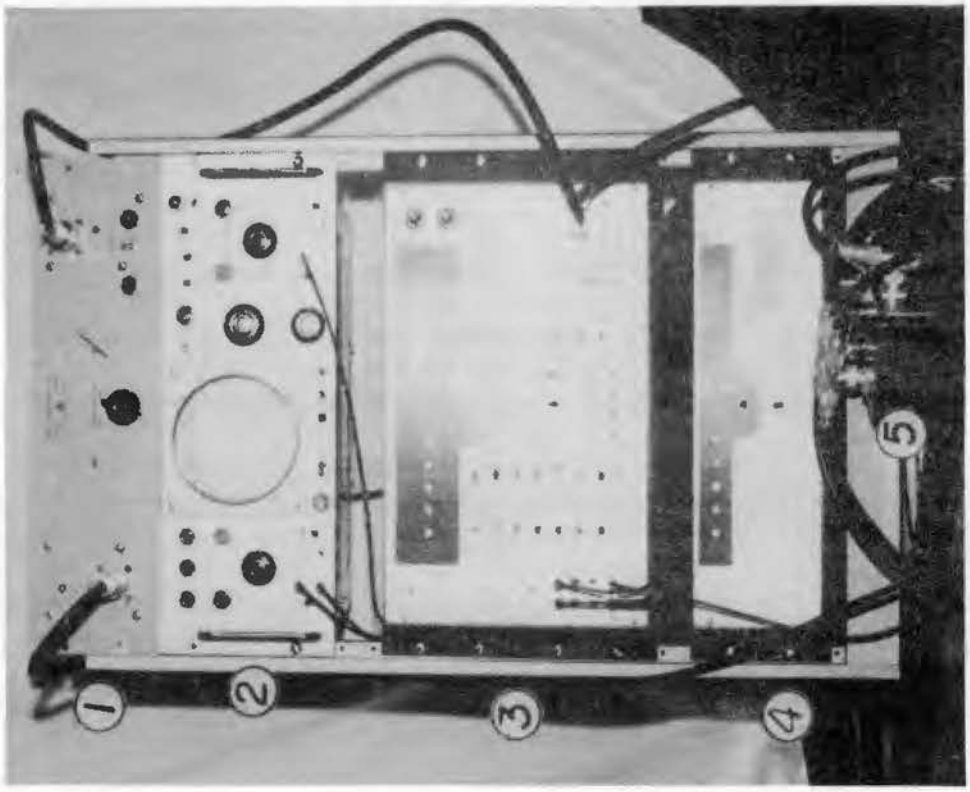
1
2
3
4
5

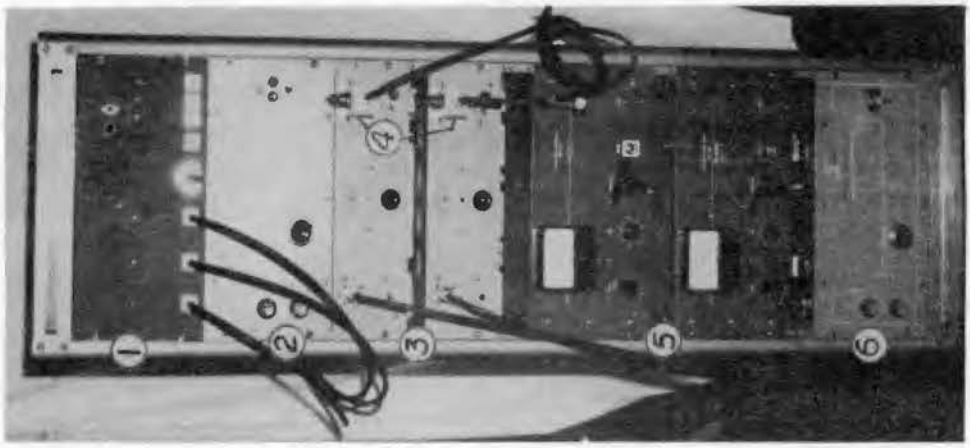
1
2
3
4
5
6

FIGURE LEGENDS

Figure 8a. Multichannel Analyser Rack

1. Hewlitt-Packard wide band amplifier
2. Tectronix 503 oscilloscope
3. Nuclear data multichannel analyser
4. Multichannel analyser power supply
5. Time-to-amplitude converter

Figure 8b. Amplifier, Power Supply Rack

1. Locally constructed triple coincidence circuit
2 & 6. Side channel discriminators and amplifier (Baird-Atomic)
3. Fast circuitry, Hewlitt-Packard wide band amplifiers
4. 404-A limiter circuits
5. Hamner high voltage photomultiplier power supplies

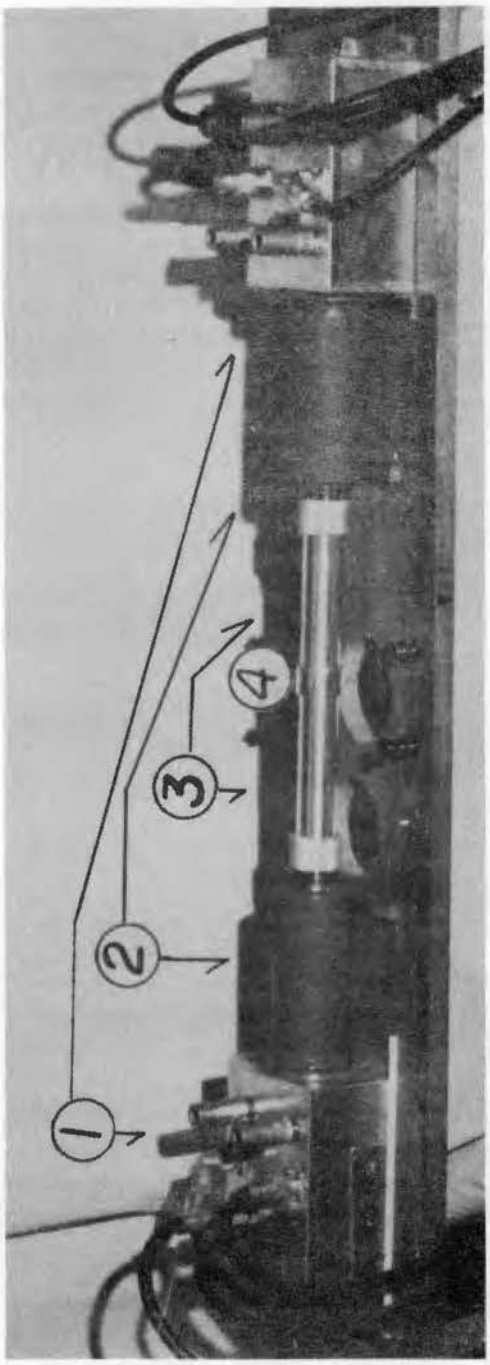
1
2
3
4

FIGURE LEGEND

Figure 9. Detector Assembly

1. Cathode follower
2. 6342-A photomultiplier
3. Ne 102 plastic fluor and light pipe
4. Aluminum retaining ring sandwiching source with aluminum samples

converter was varied in the 0.51 Mev channel. If the two events were simultaneous and the cable in one channel were lengthened, the pulse overlap time would be reduced so that the output amplitude would be reduced a corresponding amount. The multichannel analyzer sorts the pulses according to amplitude. Hence, the curve would be displaced to the left. The calibration curve (Figure 10) was then obtained by plotting peak channel number vs. inserted cable length. The "zero" time reference of the aluminum curve lies , in fact, on the centroid. Our curves were near enough to a Gaussian distribution, however, that the centroid was actually within a fraction of a channel. As will be discussed later, the stability of the equipment is plus or minus one channel; therefore, it is legitimate to use the aluminum peak channel number. The slope of the straight line was then calculated by a least mean square fit. This figure was converted from cable length to millimicroseconds by using the pulse velocity supplied by Amphenol of 25.2 centimeters per millimicrosecond. This value for the pulse velocity agrees with the value obtained by Sedlmeyer.[64]

As is indicated in Figure 10, the calibration curve flattens off at its extremes. Hence, data must be collected in the linear region of the curve. This is done by adjusting the cable delays between the limiter and the time-to-amplitude converter. No curves exhibited tails which extended into the nonlinear region.

The percentage of deviation in the calibration curves was deduced from the standard error of estimate of the data points from the best straight line. This percentage was always between 1.5% and 3.5% with the largest bulk of the data taken with the figure 1.5%.

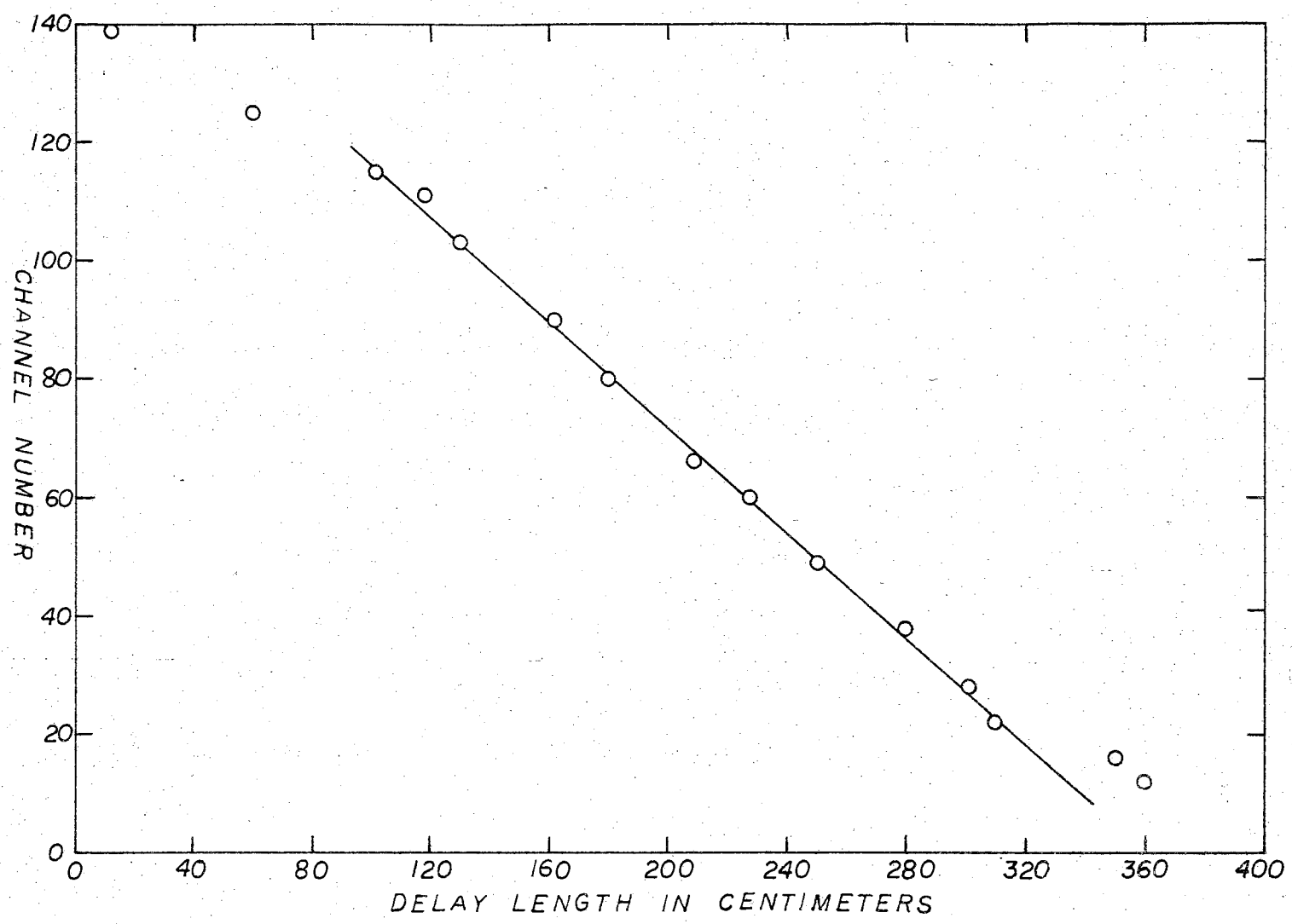

Figure 10. Calibration Curve. Least Squares fit gives 0.0890 channels/ns. Linear Region extends from channel 20 to 120.

F. Resolution

The electronic resolution of the apparatus, exclusive of the detectors, was obtained by driving both channels with the same photomultiplier output. The true intrinsic electronic curve is obtained by driving the apparatus with an impulse generator. However, a generator capable of nearly infinite rise (10^{-10} seconds) was not available. Judging by the results of others, the electronic resolution obtained using a single photomultiplier is longer than that obtained by an impulse generator by a factor of two. The width at half maximum of this curve was 0.44 millimicroseconds. The overall coincidence resolution was obtained by measuring the width at half maximum of a prompt Co^{60} source. This value was 1.10 millimicroseconds. The difference between these measurements illustrates the limit in time resolution is primarily one of the radiation detectors at the present time. The resolution time for aluminum is 1.38 millimicroseconds. These data are illustrated in Figure 11.

G. Overall Stability

(1) Short Range Stability

Short range stability studies were conducted by running aluminum curves at four hour intervals over 24 hour periods. It was found that a shift in the peak in the aluminum curve occured of $\pm$ 1 channel. This corresponds to a variation of $\pm$ 0.089 millimicroseconds.

The most likely cause was thought due to temperature fluctuation as both the photomultiplier and time-to-amplitude converter are quite temperature sensitive. A temperature variation between 23.0°C and 23.7°C

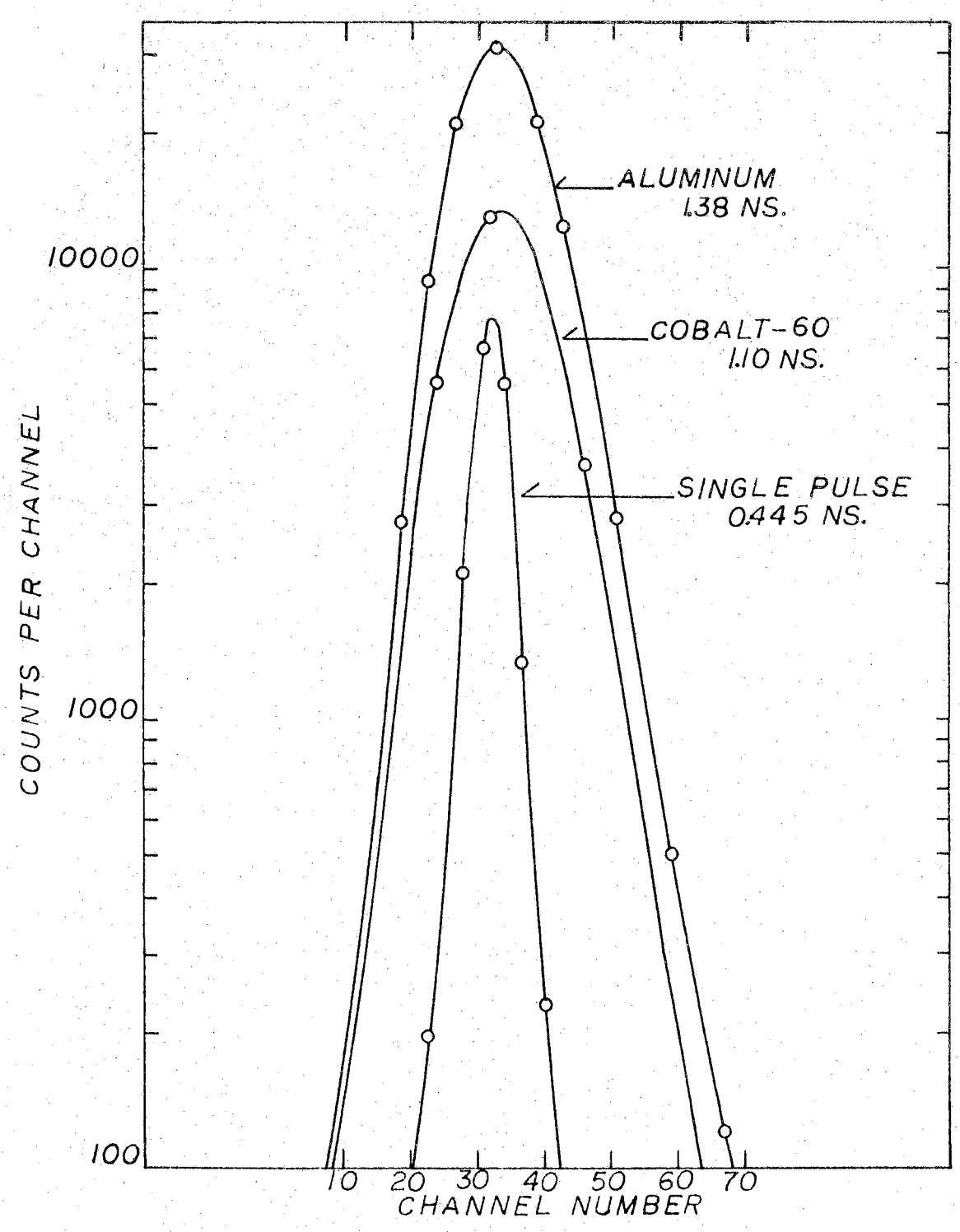

Figure 11. Resolution Curves.

was recorded over the 24 hour periods in the air conditioned laboratory. However, there appeared to be little or no correlation between the temperature and the peak channel fluctuations.

Line voltage changes are also subject to suspicion in regard to these shifts. A variation of $\pm$ 2 volts was found to occur over a 24 hour period at the output of the Sorensen regulator but no noticeable effect was observed at the photomultiplier power supplies or time-to-amplitude converter bias. Additional protection is available here, however, as the power supplies also contain internal voltage regulators. No correlation was evident between line voltage and peak channel number.

The limiter current is also an extremely sensitive parameter as this current determines the bias on the integrating transistor in the time-to-amplitude converter. However, this effect was not studied as errors due to short range drift are an order of magnitude smaller than the positronium lifetime. Consequently, little effort was given to isolating this drift. However, a precaution to minimize this effect was taken in that no data were collected over a period of time greater than eight hours, thereby decreasing the chance of a full two channel shift.

(2) Long Range Stability

At various intervals (usually of about three weeks) a few points of the calibration curve were rechecked and the points checked always lay within short range drift effects of the calibration curve.

It was found necessary, however, to recalibrate the system if the power was ever turned off. Consequently, the power was left on continuously if at all possible.

H. Counting-Rate Effect

The counting-rate effect is a consequence of fatigue of the final stages of the photomultiplier tube due to too closely bunched pulses. This effect can be eliminated by (1) using low activity sources and (2) decoupling the latter photomultiplier dynodes with capacitors. Both of these precautions were, of course, taken. Figure 12 illustrates the counting rate effect for aluminum. The resolution (width of curve at half-maximum) is not noticeably affected by the counting rate nor is the centroid of the curve. At the base of the curve, however, the slower rate curve is somewhat narrower. There is no evidence, however, that this effect alters the value of $T_{\frac{1}{2}}$. In these data the same geometry was used consistently for each material--slow-rate geometry for organic wax and polyethylene and fast-rate geometry for borax. This effect might be eliminated by the use of a pile-up detector.

I. Preparation of Samples and Sources

(1) Aluminum

The sodium-22 source used for the aluminum sample was prepared as follows: A 5 microcurie drop of a .5 to 1 millicuries per milliliter $Na^{22}Cl$ solution was deposited on a thin mylar foil of 2 mil. thickness. The $Na^{22}Cl$ solution has a specific activity of 1 ml/mg of sodium and was supplied by United Kingdom Atomic Energy Authority (Amersham, England.)

The water was then evaporated by means of a heating lamp. Another mylar foil was then placed atop the first and this sandwich was fixed very tightly by an aluminum retaining ring 1 3/8 inches in diameter. (See Figure 13) The retaining ring was designed so that it would slip

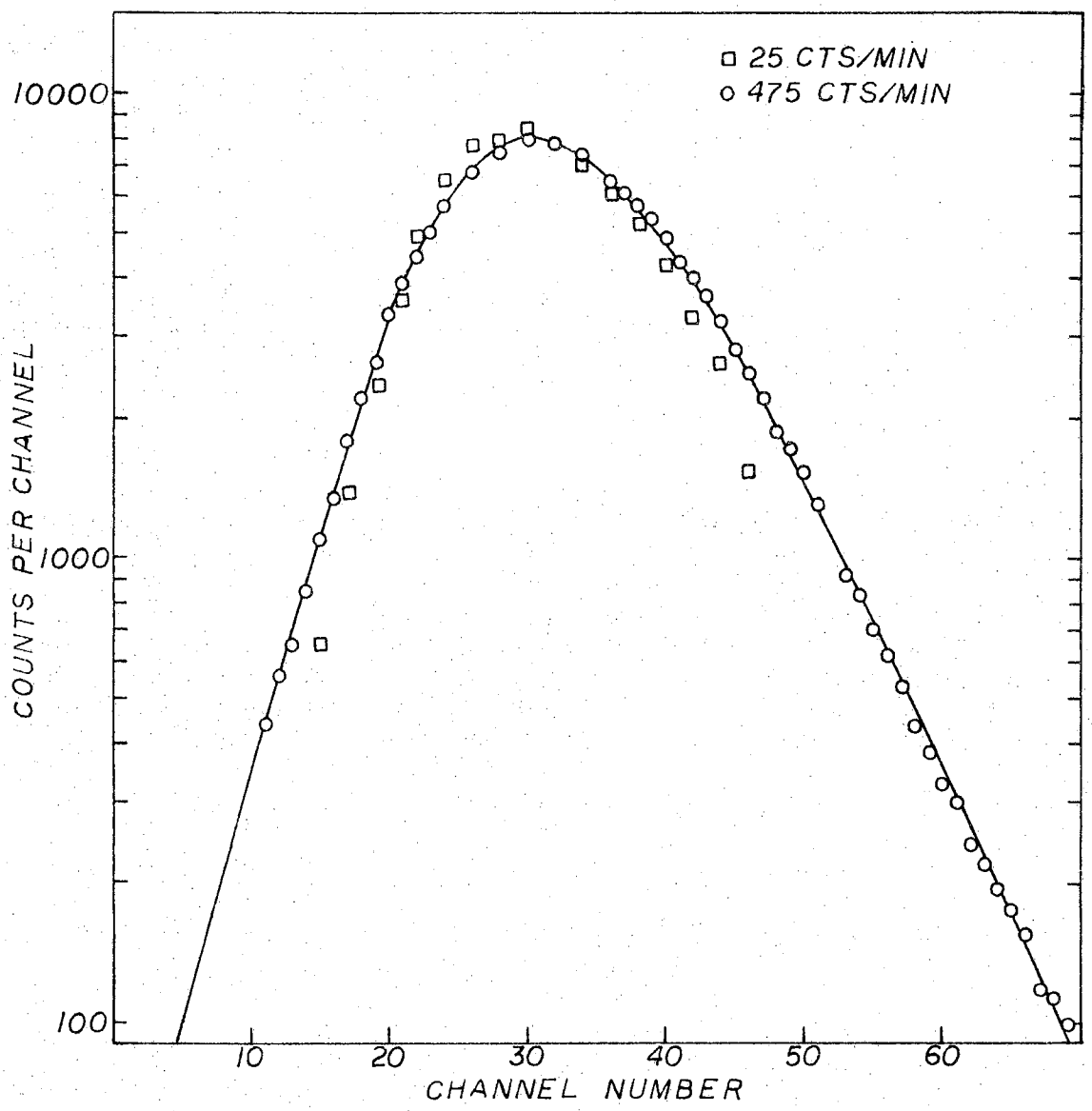

Figure 12. Counting-Rate Effect Curves.

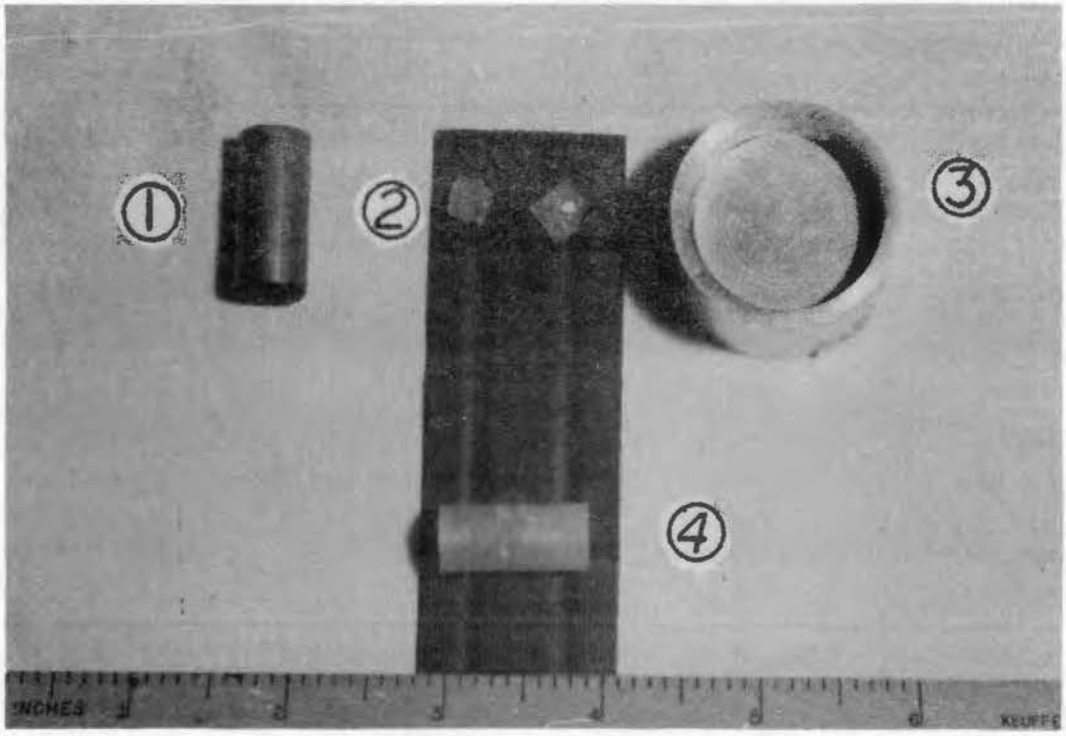
①
②
③
④
INCHES
KEUFFEL

FIGURE LEGEND

Figure 13. Samples and Sources

1. Brass cylinder containing organic wax sample with self enclosed source.
2. Borax samples.
3. Aluminum retaining ring with mylar sandwich. $Na^{22}Cl$ is in center of sandwich.
4. Polyethylene sample with self enclosed source.

over the fluor holder snugly as in Figure 9.

The aluminum samples were cut into discs which had a diameter equal to the inside diameter of the ring and a thickness of 1/10 inches which is sufficient to stop the most energetic positrons from Na^{22}. The aluminum discs could then be placed tightly against the mylar sandwich and the fluors placed next to the aluminum. The final physical layout may be seen in Figure 13.

(2) Borax

Two fused borax samples were made by different methods. The first technique was to heat commercial cleansing borax above its melting temperature (770°C) in an oven and allowing it to cool very slowly so as to prevent cracking. This method turned out to be quite cumbersome as a cruicible with the same temperature expansion coefficient as borax was not readily available and the borax cracked upon cooling. However, uncracked pieces large enough to serve as samples remained. In the second, and much easier method, the fused borax samples were made by melting powdered borax in a carbon mold by means of an acetylene torch.

Once the fused pieces were obtained, one surface was smoothed with fine emery cloth, so that these samples could be placed tightly between the mylar sandwich containing the source and the scintillator housings.

The first set of samples were made from commercial cleansing borax (99%) and the other set was made from reagent grade (99.99 5%) sodium borate.

(3) Polyethylene

The polyethylene samples were prepared as follows. The polymer was machined in two cylinders, 5/8" length by 0.438" diameter. One of

these cylinders then had a cylindrical depression cut in the center of one end while the other was machined on an end to a stud which would tightly fit into the depression of the first cylinder filling all space. The $Na^{22}Cl$ solution was deposited in the cavity. The water was evaporated by means of a heat lamp and the cylinders were force-fit together. As a further precaution, the parts were fixed with an epoxy resin. The final size of the sample was 1" x .438. See Figure 13.

(4) Organic Wax

The organic wax selected was a brittle, high temperature wax called Apiezon "W" (distributed in the U.S.A. by James G. Biddle Co., 1316 Arch Street, Philidelphia 7, Penn.). The apiezon sample was prepared in a manner similar to the polyethylene. A cylinder of similar dimensions to the polyethelene was halved and the bottom was inserted quite tightly into a brass cylinder whose inside dimensions equalled that of the wax. The $Na^{22}Cl$ was deposited in as small a drop as possible on the center of the half-cylinder and dried. The other half of the cylinder was then pressed very tightly over that already in place so that no air space could remain in the compound. See Figure 13.

J. Construction of Low Temperature Apparatus

Design of the low temperature apparatus was instituted by colleague Robert Eagleton[65] and special consturction problems are discussed in his thesis.

A special dewar was made in which the source could be placed in a flattened bulb to give optimum geometrical arrangement. (See Figure 14(a) The remainder of the bulb and the cylindrical portion of the dewar were then filled with either liquid nitrogen, dry ice, or ice water, holding the temperature constant at -195.8, -78.5 and 0°C respectively.

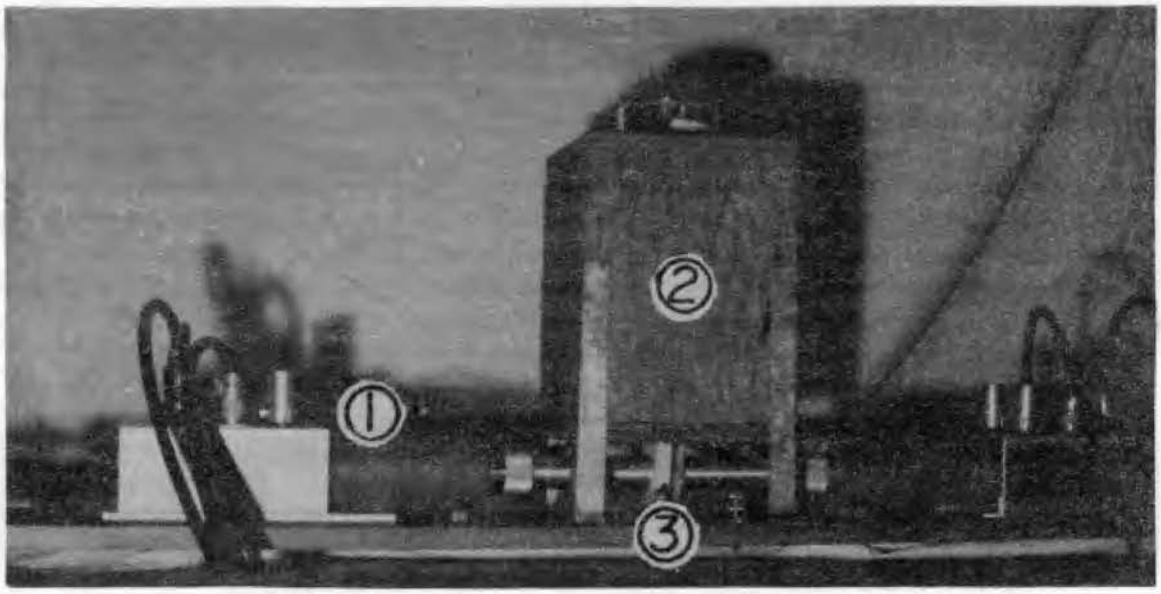
①
②
③

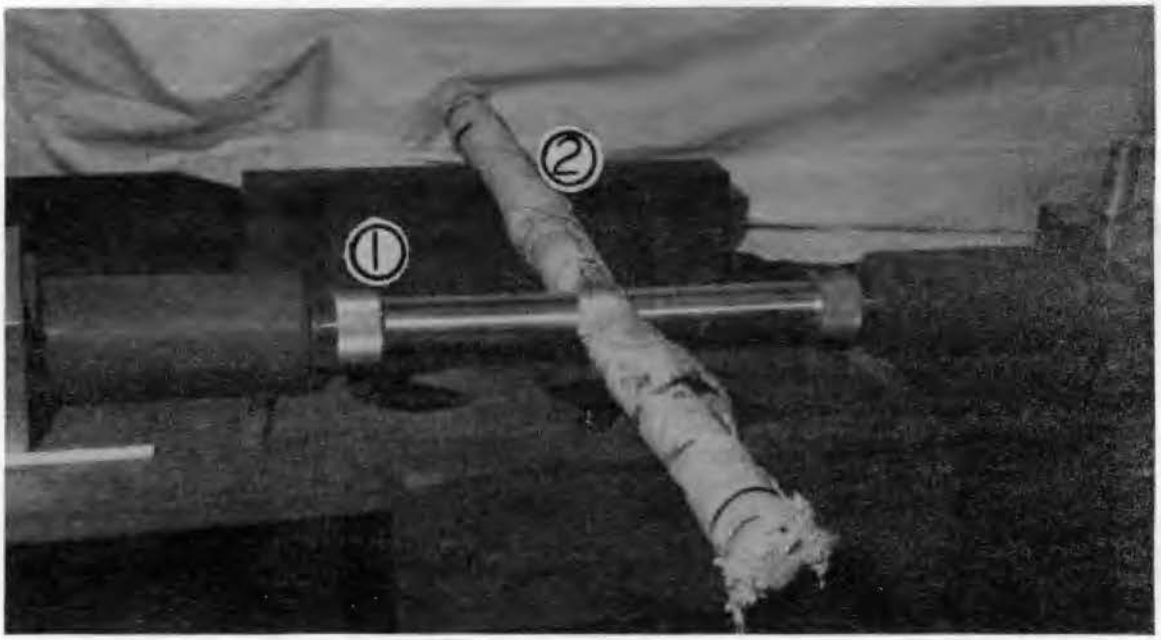
①
②

FIGURE LEGENDS

Figure 14a. Low Temperature Apparatus

1. Detector assembly (See Figure 9 for detail).
2. Plywood dewar stand. Note dewar at top.
3. Sample holder in bottom of dewar.

Figure 14b. High Temperature Apparatus

1. Detector Assembly.
2. Heating rod, wrapped in asbestos. Sample is between fluors in center of rod.

The inside separation of the flattened portion was slightly greater than 0.500 cm. so that the sample holding brass cylinders would not break the dewar upon expansion.

K. Construction of High Temperature Apparatus

The high temperature apparatus was designed by colleague Gerald Loper[66]; construction problems and calibration data may be found in his thesis.

The heater was a copper rod 1 inch in diameter by 31 inches length. A hole corresponding to the diameter of the sample holding cylinders was drilled in the center of the rod so that the sample could be completely embedded in the heater.

The heating element was made by encasing 26 gauge chromel wire in Sauereisen Electric Resistor Cement, No. 28 Paste (Sauereisen Cements Company, Pittsburgh 15, Pennsylvania). A three feet length of the resistance wire (0.214 ohms per inch) was wrapped around the rod on each side of the sample cavity and these were wired in parallel to a D.C. current source.

The entire assembly was then wrapped with asbestos tape.

As an example of the power necessary to operate this apparatus, to achieve a temperature of 40°C in this work a potential of 17 volts was needed, thus requiring 4.4 amperes.

The temperature in the sample is measured by means of an iron-constantan thermocouple which was inserted directly into the sample. Control was achieved manually.

CHAPTER IV

RESULTS AND CONCLUSIONS

A. Electronic System

(1) Results

The electronic system proved to be quite adequate to measure the anomalous T_2 component. Comparison of the resolution time of the system used in this work with other systems which are often quoted in the literature bears this out.

TABLE I

RESOLUTION TIME ACHIEVED BY VARIOUS EXPERIMENTERS

Experimenters	Resolution	Reference
Bell & Graham	2. ns	9
Bell & Green	1.4 ns*	27
deBenedetti & Richings	2. ns	10
Gerholm	2. ns*	28
Hogg, et al.	2.2 ns	67
Ferguson & Lewis	2. ns	68
Bell & Jørgensen	0.5 ns	69
This work	1.1 ns	--

*Not given explicitly, but calculated from graphical data.

The system of Bell and Jørgensen was used exclusively to measure the T_2 of metals.

Another quite desirable feature is the confidence factor assigned to the calibration factor (millimicrosecond per channel). The only such datum recorded in the literature is found in Bell and Jørgensen's

article in which they quoted 3%. As mentioned, the system in this work varied between 1.5% for the best calibration (the one used in the large bulk of the data) to 3½%. This figure varied as it was necessary to recalibrate whenever the power was turned off, thereby causing calibration figures to change during the course of the work.

(2) Suggestions for Further Work

Figure 11, Chapter 4, which shows the resolution of the apparatus to a single pulse in comparison to a coincidence pulse, suggests that the largest part of the "smear" originates in the photomultiplier detector. Therefore, further instrumental improvements should start in this component. Currently under consideration is a detector utilizing a Phillips 56 AVP photomultiplier and a fast liquid scintillator (Nuclear Enterprises,Ltd) with good high temperature characteristics. The decay time of the liquid scintillator is considerably less than the present plastic scintillators. However, fast decay liquid scintillators are generally characterized by much lower pulse height outputs than plastic flours. The 56 AVP photomultiplier tube, however, has a gain of 10^8 at 2000 volts and may be run at 3500 volts so higher gain may be achieved. With these characteristics, it will be possible to go directly from the photomultiplier tube through a limiter to the time-to-amplitude converter, thereby eliminating the amplifier. However, an equally important aspect of the new detectors is the expected improvement of the peak-to-background ratio (see AppendixI.) The 56 AVP photomultipliers can be expected to give higher amplitude pulse outputs than the present system without applying maximum allowable potential across the tube. The signal-to-noise ratio should, therefore, be improved considerably. Further, the important time characteristics quoted by

Phillips for this tube are: rise time, 2.0×10^{-9} seconds; transit time, 3.0×10^{-10} seconds; pulse width at half height, 2.0×10^{-9} seconds.

The other critical component in the system is the time-to-amplitude converter. The Zener diode is especially critical as it establishes the bias on the transistor bases. Since semiconductors are in general quite temperature sensitive, it is felt that this assembly should be further insulated from the temperature fluxuations in the room. The simplest manner in which this could be achieved is to encase the aluminum time-to-amplitude converter chassis in styrofoam or another suitable insulator.

B. Borax

(1) Results

These measurements show a τ_2 component in fused borax which depends on the composition and the method of preparation and an intensity which is even more strongly related to these factors. One of our samples shows good agreement with Bell & Graham,[9] while the other sample raises some interesting questions.

TABLE II

RESULTS OF BORAX MEASUREMENTS

	τ_2 (n.s.)	I_2 (%)
Bell and Graham	.87 ± .5	32 ± 5
Sample #1	.73 ± .07	37 ± 5
Sample #2	1.19 ± .1	6 ± 5

(2) Discussion

As previously mentioned, Sample #1 was made in an oven from commercial borax advertised as 99% pure. This sample was slow-cooled although

subjected to the thermal stress of a crucible whose coefficient of expansion differed somewhat. Sample #3 is composed of reagent grade borax and the method of preparation was to fuse in a carbon mold with a welders torch. Bell and Graham also used this latter method although no mention of the original composition is made.

In Bell and Graham's original work, the intensity of three other samples was calculated: Fused Quartz (36%), polyethelene (29%), and polystyrene (36%). For a large number of other samples, they noted that the intensity seemed "consistent" with the figure of $\sim$30%. Other workers added benzene (31 $\pm$ 3)% and substantiated the previous results of Bell & Graham.

The first indication that this ratio was not uniform came from Landes et al.[63] who found that I_2 is quite different in molten naphthalene (29%) and crystalline naphthalene (9%). (Colleague R. Eagleton[65] found an intensity of 8% in amorphous naphthalene.)

Green and Bell[27] then set out to study this variance in fused quartz. In pure fused quartz they obtained a value of I_2 = (53 $\pm$ 8)% and by using an impure quartz quoted a value (29 $\pm$ 5)%. The obvious conclusion was then that the samples of "fused quartz" one finds in the laboratory are not well defined in composition. Taken with the variability in structure caused by the method of preparation of the quartz, it is not surprising that the values of τ_2 and I_2 should be found to vary with different samples.

With this view, we are not without precedent in quoting a different value of τ_2 and I_2 for the same material. From the theory, also, we recall that the result of ordering the structure is to decrease the Ore gap thereby reducing the probability of positronium formation.

Furthermore, the impurities usually found in borax (calcium, iron, sulfate) are higher group elements and contribute electrons very near the conduction band in the solid. These electrons have much more freedom to interfere with the positronium formation than do the normally shared electrons.

However, with this picture we would be led to say that sample #3--which has fewer impurities and which, we might be intuitively led to believe, has less order due to its rapid cooling--would exhibit the higher intensity but such is not the case. The fact that it has a value of τ_2 somewhat higher, however, is going in the expected direction as the smaller electron density allows the positronium to live unmolested longer.

The conclusion that must follow to be consistent with our theoretical picture is that the samples fused with a welders torch are actually more crystalline than those which were rate-control cooled. This perhaps arises as a result of the thermal stress placed upon the sample in cooling due to the glazed porcelain crucible. See Figure 15.

C. Polyethylene

(1) Results

Data were taken at the following temperatures: -195.8°C, -78.5°C, 0°C and 23°C. Our results compare favorably with those of Bell & Graham at room temperature. The results are:

TABLE III

RESULTS OF POLYETHYLENE DATA

Temperature	τ_2 (ns.)	I_2 (%)
-195.8	1.08 ± .1	23. ± 5
- 78.5	1.27 ± .1	22. ± 5
0	2.04 ± .1	13. ± 5
23.0	2.60 ± .06	19. ± 5

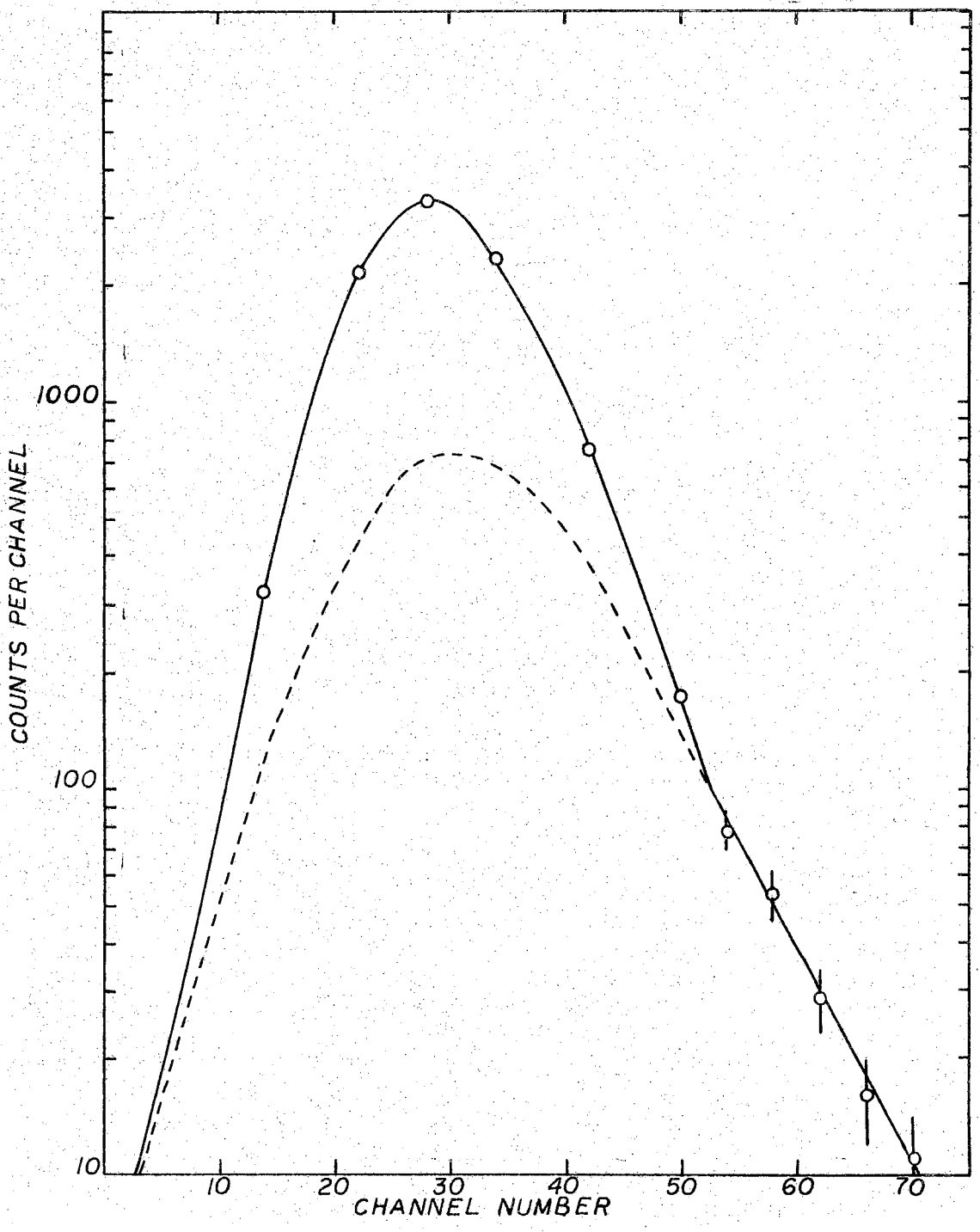

Figure 15. Experimental Borax Curve. Calibration Factor 0.0890 channels/ns.

Bell and Graham quoted: $\tau_2 = 2.4 \pm .3 \times 10^{-9}$ seconds at 23° with $I_2 = (29 \pm 5)\%$.

(2) Discussion

Several interesting features are involved in the ethylene polymer and these merit some discussion. The polymerization of ethylene in suitable high pressure conditions gives very long chain hydrocarbons. The cell dimensions and atomic positions have been established by Bunn[70] who has also observed that the crystallinity is incomplete at ordinary temperatures, for the x-ray photographs show a band due to the presence of amorphous materials. The intensity of this band increases and that of the crystal structure lines decreases with rising temperature until finally, at some temperature in the neighborhood of 120-130°C no trace of crystallinity remains.

The amorphous and crystalline regions cannot be regarded as mechanically separable phases, since it is an essential point of the theory that the same molecule may at the same time be in the crystalline condition over part of its length and over the remainder in the amorphous state. With rising temperature, increased thermal motion will cause a growth of the amorphous regions at the expense of the crystalline regions until a temperature is reached at which the material is entirely amorphous and indistinguishable from a viscous liquid composed of long molecules. Measurements of density variation with temperature give an indication of the relative proportions of the crystalline and amorphous regions and how they change the foregoing properties are suggestive of another application of positronium annihilation studies. Since the long component lifetime is dependent on the density also, it could possibly serve as a tool to determine the

percentage of crystallinity. These T_2 measurements are presently easier to perform than those the polymer chemists use in this application. The observed shape of the temperature vs. specific volume curve has the following general appearance. From liquid nitrogen to almost the brittle point, the curve is very nearly a straight line. A rather marked bend upward occurs in this region of transition temperature. From the transition temperature to approximately room temperature, the curve is again rather linear. From room temperature upward, the sample undergoes very slight volume changes, giving the curves a pronounced concavity upwards. In the subnormal temperature range there are signs of a transition occuring at about -40°C in most samples, although Selker et al.[71] have found a variation in this phase transition from -15° to -68.5°C. This transition may be interpretted as the temperature at which the amorphous material becomes "frozen" and below which expansions or contractions have the magnitude to be expected from a structure in which diffusion processes are negligible. It is not clear how the lower brittleness temperature of long chain material is to be explained simply in terms of the freezing of movement in the amorphous regions which are likely to contain only segments of molecules and thus to have properties relatively independent of specimen molecular weight.[72] Alfrey et al.[73] have also observed that the specific volume in the lower temperature range depends on the rate at which the sample was cooled. They explain the transition as a change from conditions in which, because of the higher temperature, diffusion of the long molecules is sufficiently rapid for the liquid to follow its equilibrium structure on cooling to conditions in which, because of the lower temperature, diffusion is extremely slow

and the liquid is unable to attain its equilibrium structure though being "frozen" in a less compact arrangement. The rapid cooling procedure is known as "shock cooling."

(3) Conclusions and Suggestions for Further Measurements

The plot of the data in Figure 16 might be interpreted as two rather smooth lines with a rather sharp break in the region of -40°C to -60°C. This is consistent with the phase transition just discussed. Obviously, more data need to be taken in the region between -80°C and 0°C. Such measurements would be relatively easy to make with existing facilities as there are numerous organic compounds which melt in this region that could be used in the dewar as a temperature regulator. Enough points should be taken until the phase transition is isolated. The temperature at which this occurs could then be compared to the brittle point, which is measureable by mechanical means. Also, plans are currently underway for the higher temperature measurements to be continued as part of this positron work. However, a heating system superior to the one presently employed will be necessary before approaching the high temperature phase transition. The current regulation at 100°C is about ± 4°C. A hysteresis effect can be expected in the polyethylene at this transition and data taken under such conditions would be rather questionable. Landes discussed such problems with naphthalene in his Ph.D. dissertation.[63]

Two runs were made at liquid nitrogen temperature. In the first, the sample was simply dropped into the liquid gas thereby "shock" cooling it. The $T_{\frac{1}{2}}$ for this run was $(.96 \pm .06) \times 10^{-9}$ seconds. Secondly, the sample was first cooled to dry ice temperature and then worked very slowly into the nitrogen by gradually "quick dipping" a

progressively larger portion into liquid. The τ_2 for this run was $(1.2 \pm .07) \times 10^{-9}$ seconds. The intensity in each case was 23%. In the second method the outer surface was probably shock cooled also, but it is hoped that the interior molecular chains might have had time to diffuse to equilibrium before being "frozen." See Figure 17.

D. Organic Wax

(1) Results

Data were collected at four temperatures. At -78.5°C no τ_2 was observed. The other three points are listed in Table IV.

TABLE IV

RESULTS OF ORGANIC "APIEZON W" WAX

Temperature	τ_2 (ns)	I_2 (%)
0°C	(0.97 ± 0.1)	21 ± 5
23°C	(1.31 ± 0.07)	16 ± 5
39.4°C	(1.99 ± 0.1)	11 ± 5

(2) Discussion

Scarcely enough data are available to draw any concrete conclusions regarding the behavior of positronium in Apiezon W. The manufacturer was unable to supply information on the density of the wax below 25°C. At 25°C the density is 1.055 and increases uniformly at a rate of 0.0006 per degree centigrade. The τ_2 component is plotted as a function of temperature and density in Figure 18. The dashed line indicates that the density is uncertain in this region. Another question is posed by the intensity values. At -78°C no I_2 was observed, but at 0°C the intensity is decreasing, apparently uniformly, with temperature. At

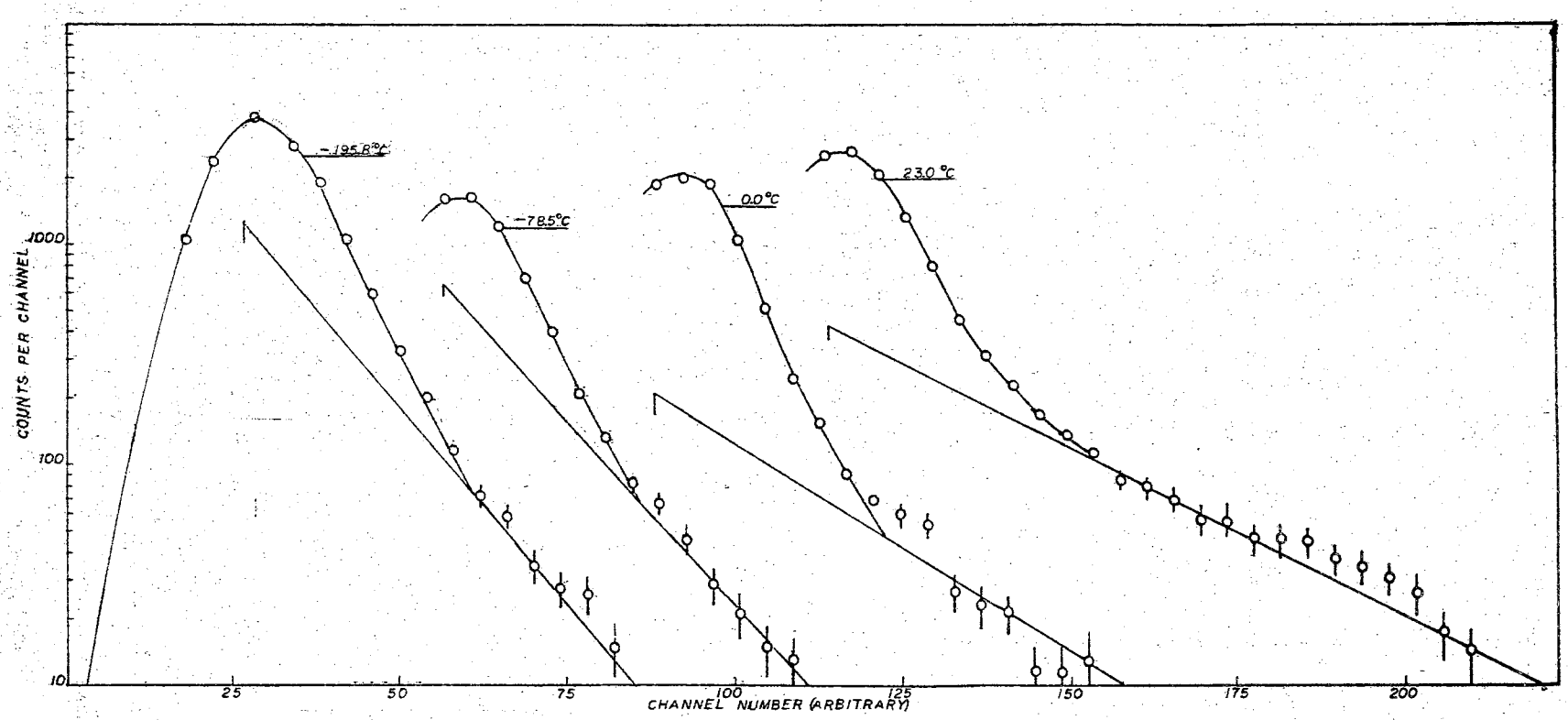

Figure 16. Experimental Polyethylene Curve. Calibration factor 0.0996 channels/ns., all others are 0.0890.

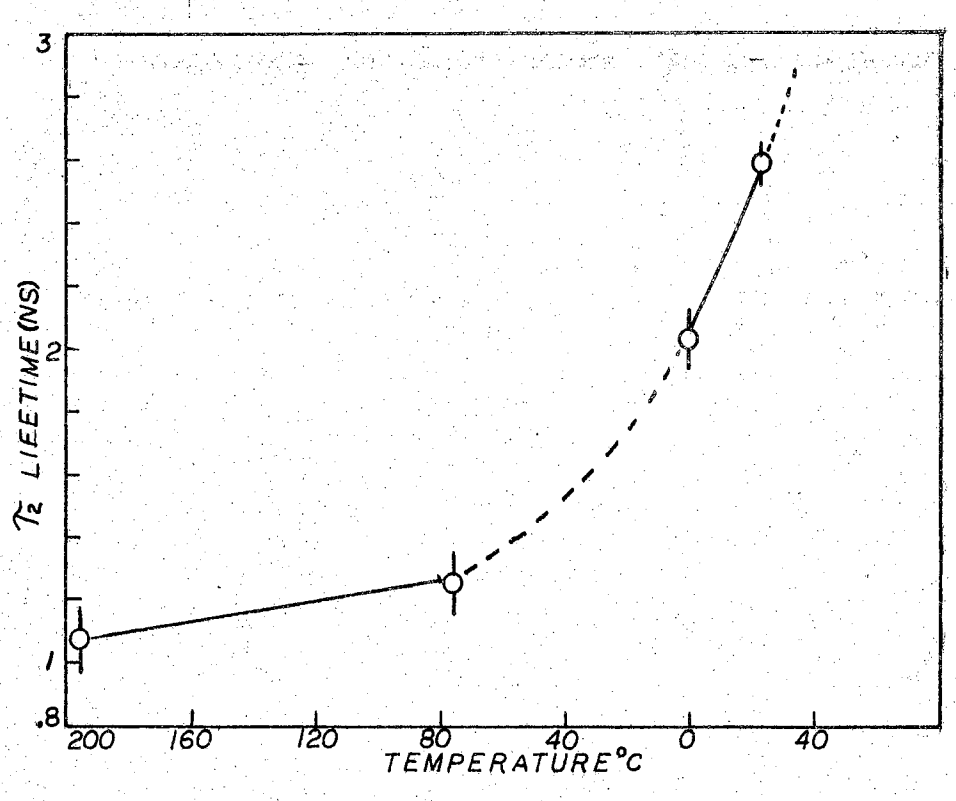

Figure 17. Variation of τ_2 with Temperature in Polyethylene.

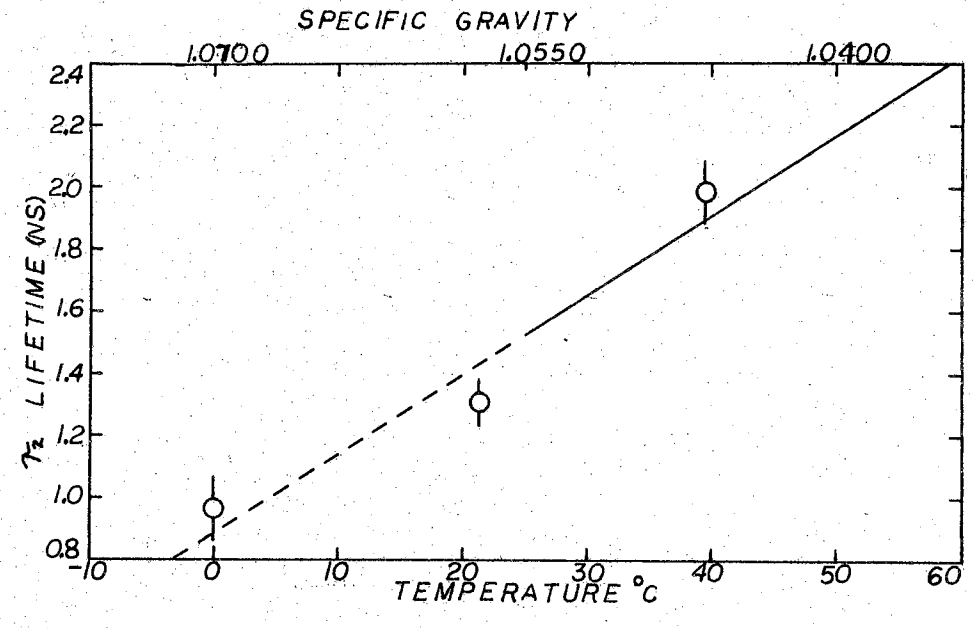

Figure 18. Variation of τ_2 with Temperature in Apiezon.

what point between -78.5°C and 0°C does this trend reverse and why? A solution as to why little, if any, positronium is found at -78.5°C probably lies in the fact that the free volume is so small that there is simply not room for positronium to form. The experimental curves are shown in Figure 19.

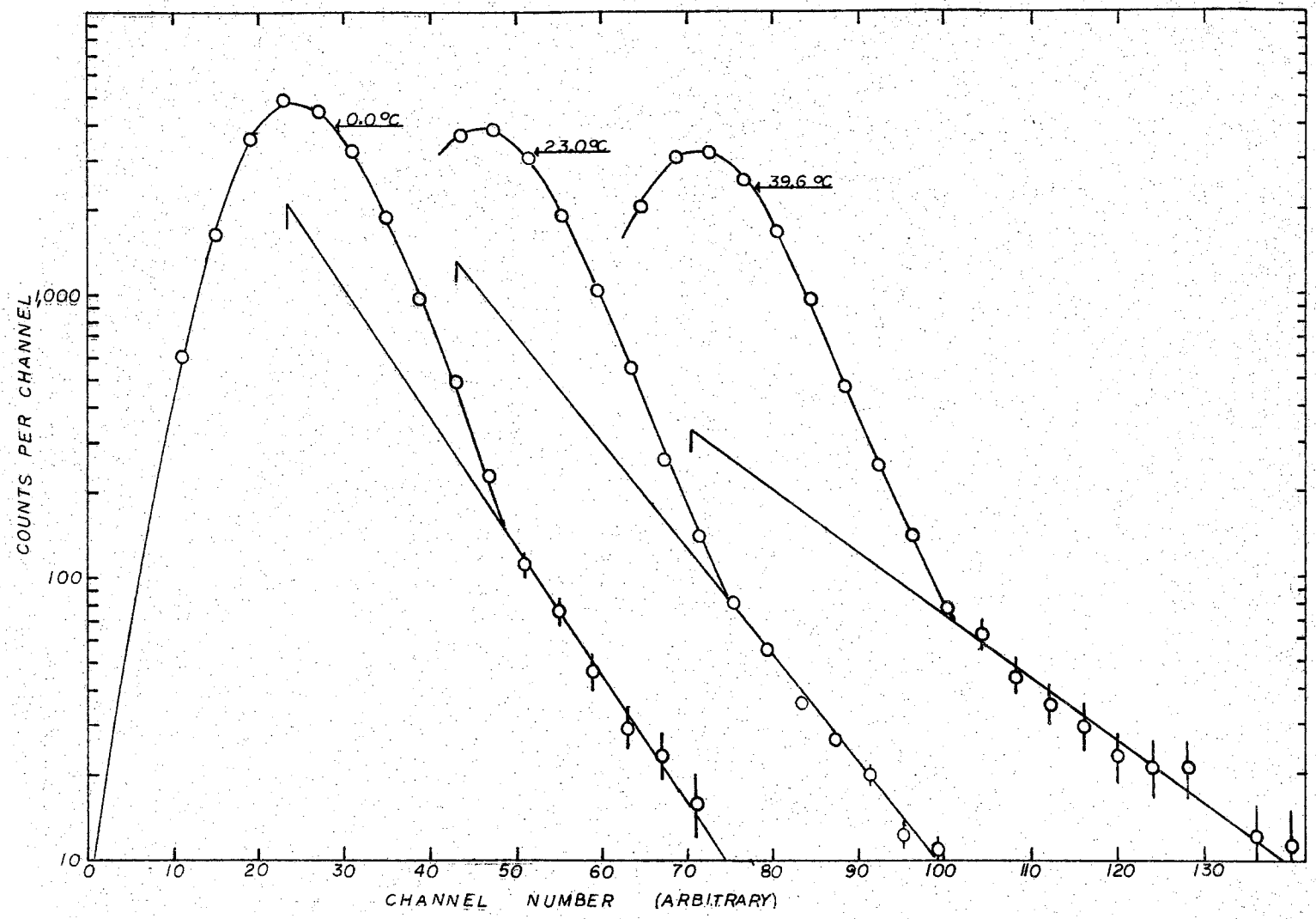

Figure 19. Experimental Apiezon Curves. Calibration factor 0.0996 channels/ns.

LIST OF REFERENCES

1. P.A.M. Dirac, Proc. Camb. Phil. Soc., 26, 361 (1930)
2. J. W. Shearer and M. Deutsch, Phys. Rev., 76, 462 (1949)
3. J. A. Wheeler, Ann. N. Y. Acad. Sci., 48, 219 (1946)
4. J. Pirenne, Arch. Sci. Phys. et. Nat., 28, 273 (1946); 29, 121, 207 (1947)
5. T. A. Pond, Phys. Rev., 85, 489 (1952)
6. A. Ore and J. L. Powell, Phys. Rev., 75, 1696, 1963 (1949)
7. S. deBenedetti and R. Siegel, Phys. Rev., 85, 371 (1952); 87, 235 (1952)
8. J. Wheatly and D. Halliday, Phys. Rev., 88, 424 (1952)
9. R. E. Bell & R. L. Graham, Phys. Rev., 90, 644 (1953)
10. S. deBenedetti and H. J. Ritchings, Phys. Rev., 85, 377 (1952)
11. G. Hinman, D. Brower, and R. Leamer, Phys. Rev., 90, 370 (1953)
12. V. F. Weiskopf, Phys. Rev., 83, 1073 (1951)
13. S. A. Moszkowski, Phys. Rev., 83, 1071 (1951)
14. A. W. Sunyar, Phys. Rev., 98, 653 (1955)
15. D. K. Alkhazov et al., Sov. Phys. J.E.T.P., 9, 222 (1959)
16. S. deBennedetti et al., Phys. Rev., 77, 205 (1950)
17. R. L. Garwin, Phys. Rev., 91, 1571 (1953)
18. G. E. Lee-Whiting, Phys. Rev., 97, 1557 (1954)
19. J. W. M. DuMond, D. A. Lind, and B. B. Watson, Phys. Rev., 75, 1226 (1949)
20. A. Hedgran, Phys. Rev., 82, 128 (1951)
21. G. Lindstrom, Phys. Rev., 83, 465 (1951)

22. W. Heitler, The Quantum Theory of Radiation (Oxford), (1955)

23. J. W. Shearer and M. Deutsch, Phys. Rev., 82, 336 (1951)

24. J. Gerhart, B. Carlson, and R. Shear, Phys. Rev., 94, 917 (1954)

25. L. Mandansky and F. Rasetti, Phys. Rev., 79, 397 (1950)

26. S. deBenedetti and R. Siegel, Phys. Rev., 85, 371 (1952)

27. R. E. Green and R. E. Bell, Can. J. Phys., 36, 1684 (1958)

28. T. R. Gerholm, Arkiv Fysik, 10, 523 (1956)

29. R. E. Bell and Jørgensen, Can. J. Phys., 38, 652 (1960)

30. S. Berko and A. J. Zuchelli, Phys. Rev., 102, 724 (1956)

31. M. Deutsch, Mass. Inst. Technol., Lab. Nuclear Sci. and Engr. Progress Report, p. 178 (May, 1952)

32. E. P. Dulit, B. Gittelman, and M. Deutsch, Bull. Am. Phys. Soc. (2)1, 69 (1956)

33. J. A. Whalen, Bull. Am. Phys. Soc., (2) 1, 167 (1956)

34. Jaeger and H. R. Hilme, Proc. Camb. Phil. Soc., 32, 158 (1936)

35. R. E. Green and H. T. Stewart, Phys. Rev., 98, 486 (1955)

36. J. Des Cloizeauz and G. Ambrosino, Compt. rend., 237, 1069 (1953)

37. Lang, S. deBenedetti, and Smoluchowski, Phys. Rev., 99, 596 (1955)

38. A. T. Stewart, Phys. Rev., 99, 594 (1955)

39. L. A. Page and M. Heinberg, Phys. Rev., 102, 1545, (1956)

40. L. A. Page, M. Heinberg, P. R. Wallace, and Trout, Phys. Rev., 98, 206 (1955)

41. S. deBenedetti and R. Siegel, Phys. Rev., 94, 955 (1954)

42. H. S. Landes, S. Berko, and A. J. Zuchelli, Bull. Am. Phys. Soc. Sec. II, 1, 68 (1956)

43. R. L. Graham and A. T. Stewart, Phys. Rev., 102, 724 (1956)

44. R. T. Wagner and F. C. Hereford, Phys. Rev., 99, 593 (1955)

45. R. L. DeZafra and W. T. Joyner, Phys. Rev., 112, 19 (1958)

46. P. R. Wallace, Phys. Rev., 100, 738 (1955)

22. W. Heitler, The Quantum Theory of Radiation (Oxford), (1955)

23. J. W. Shearer and M. Deutsch, Phys. Rev., 82, 336 (1951)

24. J. Gerhart, B. Carlson, and R. Shear, Phys. Rev., 94, 917 (1954)

25. L. Mandansky and F. Rasetti, Phys. Rev., 79, 397 (1950)

26. S. deBenedetti and R. Siegel, Phys. Rev., 85, 371 (1952)

27. R. E. Green and R. E. Bell, Can. J. Phys., 36, 1684 (1958)

28. T. R. Gerholm, Arkiv Fysik, 10, 523 (1956)

29. R. E. Bell and Jørgensen, Can. J. Phys., 38, 652 (1960)

30. S. Berko and A. J. Zuchelli, Phys. Rev., 102, 724 (1956)

31. M. Deutsch, Mass. Inst. Technol., Lab. Nuclear Sci. and Engr. Progress Report, p. 178 (May, 1952)

32. E. P. Dulit, B. Gittelman, and M. Deutsch, Bull. Am. Phys. Soc. (2)1, 69 (1956)

33. J. A. Whalen, Bull. Am. Phys. Soc., (2) 1, 167 (1956)

34. Jaeger and H. R. Hilme, Proc. Camb. Phil. Soc., 32, 158 (1936)

35. R. E. Green and H. T. Stewart, Phys. Rev., 98, 486 (1955)

36. J. Des Cloizeauz and G. Ambrosino, Compt. rend., 237, 1069 (1953)

37. Lang, S. deBenedetti, and Smoluchowski, Phys. Rev., 99, 596 (1955)

38. A. T. Stewart, Phys. Rev., 99, 594 (1955)

39. L. A. Page and M. Heinberg, Phys. Rev., 102, 1545, (1956)

40. L. A. Page, M. Heinberg, P. R. Wallace, and Trout, Phys. Rev., 98, 206 (1955)

41. S. deBenedetti and R. Siegel, Phys. Rev., 94, 955 (1954)

42. H. S. Landes, S. Berko, and A. J. Zuchelli, Bull. Am. Phys. Soc. Sec. II, 1, 68 (1956)

43. R. L. Graham and A. T. Stewart, Phys. Rev., 102, 724 (1956)

44. R. T. Wagner and F. C. Hereford, Phys. Rev., 99, 593 (1955)

45. R. L. DeZafra and W. T. Joyner, Phys. Rev., 112, 19 (1958)

46. P. R. Wallace, Phys. Rev., 100, 738 (1955)

47. R. Stump, Bull. Am. Phys. Soc., (2)2, 173 (1957)

48. R. Karplus and A. Klein, Phys. Rev., 86, 257 (1952)
Weinstein, Deutsch and Brown, Phys. Rev., 94, 758 (1954)

49. R. Farrell, Rev. of Mod. Phys., 28, 308 (1956)

50. J. M. Jauch and R. Rohrlich, The Theory of Photons and Electrons, Addison-Wesley, Chap. 12, (1955)

51. A. Ore, Univ. Bergen Avhok, Naturvidenskep. Rekke, No. 12 (1949)

52. M. Deutsch, Prog. Nucl. Phys. 3, 131 (1953)

53. P. R. Wallace, Solid State Phys., 10, 1 (1960)

54. Kohonen, Ann. Acad. Sci. Fennicae, Ser. A VI, 92 (1961)

55. W. R. Dixon and L. E. H. Trainor, Phys. Rev., 97, 733 (1953)

56. R. L. Brock and J. F. Streib, Phys. Rev., 109, 399 (1958)

57. Brandt, Berko, and Walker, Phys. Rev., 120, 1289 (1960)

58. R. Post and L. J. S. Schiff, Phys. Rev., 80, 1113 (1950)

59. R. E. Bell, R. L. Graham, H. E. Petch, Can. J. Phys., 30, p. 35 (1952)

60. Lewis and Wells, Millimicrosecond Pulse Techniques, McGraw-Hill (1954)

61. G. Jones, Journ. Sci. Inst., 37, 318 (1960)

62. Simms, To be published

63. Berko and Landes, (unpublished Ph. D. dissertation, University of Virginia, (1956)

64. J. Sedlmeyer (unpublished report) Edgerton, Germeshausen, and Grier, Inc., Las Vegas, Nev.

65. Robert Eagleton, (unpublished, M.S. Thesis, Oklahoma State University, (1961)

66. Gerald Loper (unpublished, M.S. Thesis, Oklahoma State University, (1962)

67. B. G. Hogg, T. H. Sutherland, D. A. L. Paul and J. W. Hodgkins, J. Chem. Phys., 25, 1082 (1956)

68. A. J. C. Ferguson and G. M. Lewis, Phil. Mag. (7)44, 1339 (1953)

69. Bell and Jørgensen, Nuclear Physics, 12, 413 (1959); Can. J. Phys., 38, 652 (1960)

70. C. W. Bunn, Trans. Faraday Soc., 35, 482, (1939)

71. M. L. Selker, G. G. Winspear and A. R. Kemp, Ind. Eng. Chem., 34, 157 (1942)

72. E. Hunter and W. B. Oakes, Trans. Faraday Soc., 41, 49 (1945)

73. T. Alfrey, G. Goodfinger, M. Mark, J. App. Phys., 14, 700 (1943)

74. Z. Bay, et al., Phys. Rev., 100, 1197 (1955)

75. T. D. Newton, Phys. Rev., 78, 790 (1950)

76. Z. Bay, Phys. Rev., 77, 419 (1950)

77. E. B. Wilson, An Introduction to Scientific Research, McGraw-Hill (1952)

A P P E N D I C E S

APPENDIX I

BACKGROUND

Perhaps the major part of the uncertainty associated with our measurements may be attributed to the problem of background. The average peak-to-background ratio was about 610:1; however, ratios as good as 1300:1 were obtained.

Two methods were considered for calculating the background. The first of these is illustrated in Figure 20, which presents a lifetime measurement with one of our poorest peak-to-background ratios. The solid points are the actual counts per channel as given by the multi-channel analyser. The circles represent typical counts in portions of the curve for which the background discussion is irrelevant. By considering the counts in channels 100 to 128, which from the data appear to be randomly grouped around six, we may take the average and call this the background. However, 14 of these counts (or about 8%) may actually be annihilations. This figure is obtained by extrapolating the tail to one count, then adding the projected number of counts in each of the channels. Therefore, the background may be adjusted to 5.18 counts per channel. This figure may then be subtracted from all of the points and the analysis proceed by computing the least mean square fit illustrated by the dashed line. The second method consisted of delaying the 0.51 Mev channel by adding a length of cable between the limiter and the time-to-amplitude converter, which

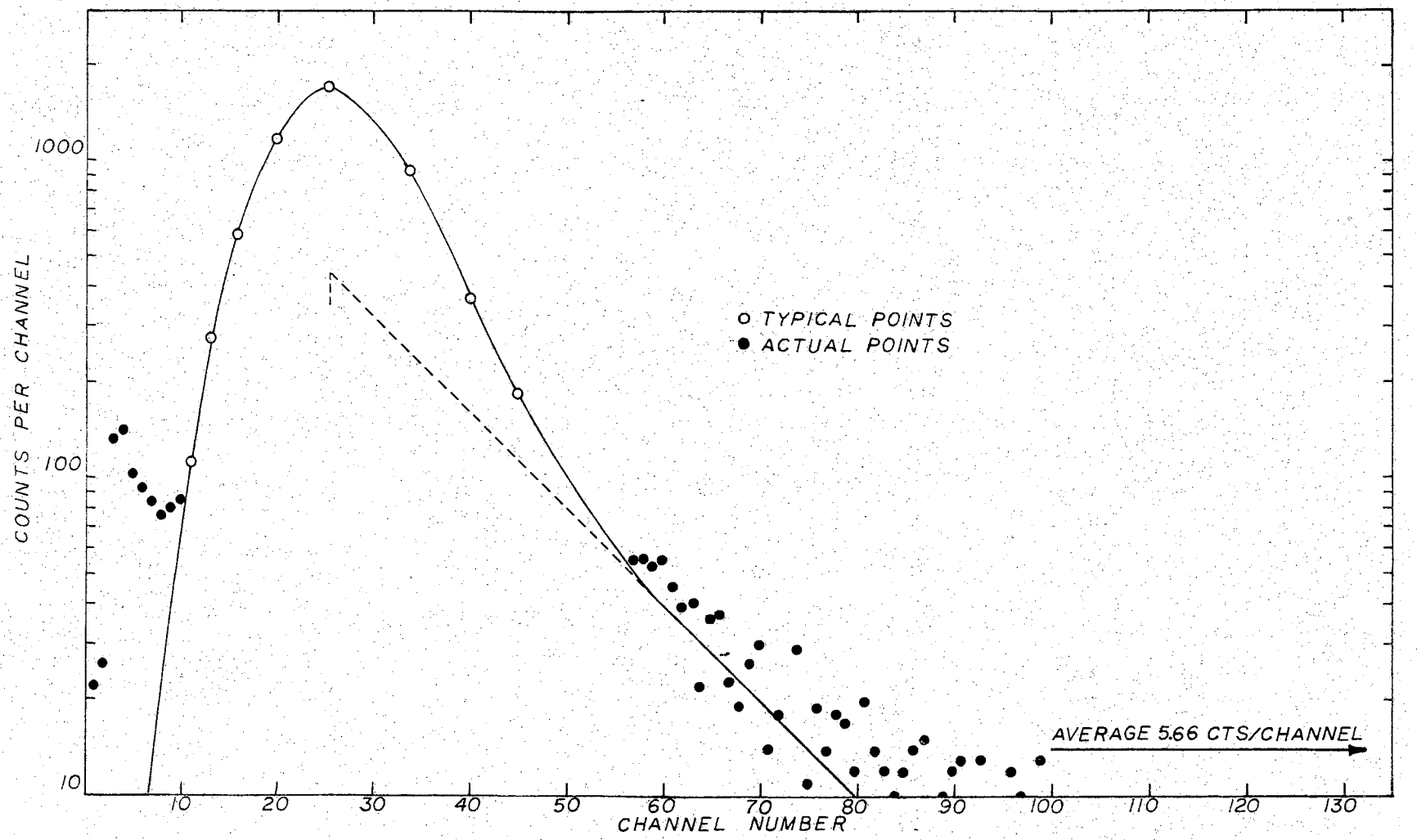

Figure 20. Background Analysis Curve.

effectively "shifts the curve off the scale" to the left. In this way, very nearly all the counts which are analyzed are not associated with either lifetime component. It would seem that the results obtained by these two methods should be about the same, but differences as large as 20% were observed. It was decided that the first method was the more reliable; consequently, if the τ_2 component were short enough (i.e., the curve steep enough) to give enough (say 20) channels of background where the straight line was below one count per channel, the first method was used. In the samples exhibiting a long lifetime component of about 1.8 μs or greater the second method was used. It is estimated that the difference in background treatments could effect the short lifetime as much as 10%, although in most cases 5% is perhaps more nearly correct.

The incertitude regarding this method, however, makes the study of τ_2 in metals most difficult with the present system.

A related problem is suggested by the data in the first ten channels of Figure 20. Due to low level noise generated in the electronics and to the nonlinearity of the converter in this region, a substantial portion of the left hand side of the curves is obtained by extrapolation.

The effect of an incorrect interpolation is felt in calculating the centroid from which τ_1 is obtained. (See Appendix II.) Although the area is only very weakly affected by a change in this portion of the curve, the moment is slightly affected. It was estimated that an error as large as 40% could occur in the τ_1 value due to this effect although 12% is a very much more reasonable estimate.

As an example of this effect coupled with the short range drift

effect (See Chapter 3) on the τ_1, we may perform the following calculation. For a τ_1 of .24 ns., 12% is .03 ns. Should a centroid shift of one channel occur due to a short range drift, and with a probable statistical error of .05 ns., the error could be

$$\sigma = \left[(.03)^2 + (.09)^2 + (.05)^2\right]^{1/2} ns,$$

$$\sigma = 0.11 ns$$

Thus, the τ_1 might be expected to vary as much as ±46%. It is for these reasons that only a passing degree of confidence is held for the experimental values of τ_1.

APPENDIX II

METHOD OF ANALYSIS

Delayed coincidence techniques, as used in the study of positron lifetime behavior, give an experimental curve which is a composite of the apparatus resolution curve and the delayed coincidence curve due to the lifetime of the positron (or curves if positron has more than one lifetime such as τ_1 and τ_2).[74-76] In order to interpret the resulting experimental curve, it is necessary to define the apparatus resolution curve, also called a "prompt" curve, which is obtained by plotting coincidences of a source of simultaneous events as a function of channel number. Whenever the drop off rate due to the coincidence apparatus is less than the mean lifetime for positrons annihilating in aluminum, the curve obtained for positrons annihilating in aluminum (after being corrected for the lifetime in aluminum) can be used as a "prompt" curve.

The equation for the delayed coincidence curve is then expressed in terms of the "prompt" curve as

$$F(x) = \int_{-\infty}^{\infty} f(t)\, p(x-t)\, dt \qquad (1)$$

where $F(x)$ = delayed coincidence curve

$p(x)$ = prompt curve (adjusted aluminum curve)

$f(t)$ = probability of a positron annihilating in an interval dt in a time t.

x = channel number

The above relation is valid if: (1) x and t are interchangeable, i.e., inserted time delay does not affect pulse shape, and (2) pulse shape distributions in both channels of coincidence circuit are the same for $F(x)$ and $\rho(x)$. Condition (1) is satisfied by using short delay cables of negligible attenuation, whereas condition (2) is satisfied by proper pulse shaping (done by Western Electric 404-A limiters in this experiment.)

Since positron lifetime decay exhibits an exponential distribution in time,

$$f(t) = \lambda e^{-\lambda t} \qquad \text{for } t > 0$$
$$f(t) = 0 \qquad \text{for } t < 0$$

so that:

$$F(x) = \lambda \int_0^\infty e^{-\lambda t} \rho(x-t)\, dt \tag{2}$$

In some cases, the "prompt" curve can be approximated quite closely with a Gaussian distribution of the form:

$$\rho(x) = e^{-h^2 x^2} \tag{3}$$

in which case

$$F(x) = \lambda \int_0^\infty e^{-\lambda t} e^{-h^2 (x-t)}\, dt \tag{4}$$

can be reduced to an error integral. The tabulated error integrals then permit the use of this analytical expression for the delayed lifetime curve.

However, at times, the prompt curve is not symmetrical and hence cannot be represented by a simple analytic function as above. Such an

assymetry could be due to the electronics-discriminator settings. The integral representing $F(x)$ is then replaced by the summation

$$F(x) = \sum_{t=0}^{n} \rho(x-t)\lambda\, e^{-\lambda t} \qquad (5)$$

The delayed coincidence curve is then folded out of the composite experimental curve, according to the above summation, by means of a numerical integration (Simpson's rule). The values for $F(x)$ so obtained, when plotted, give the delayed curve.

Differentiating the integral relation for $F(x)$ with respect to x gives:

$$\frac{dF(x)}{dx} = \lambda[\rho(x) - F(x)], \quad \frac{d\ln F(x)}{dx} = -\lambda\left[1-\frac{\rho(x)}{f(x)}\right]$$

and

$$\frac{d\ln F(x)}{dx} = -\lambda \quad \text{when } F(x) \gg \rho(x) \qquad (6)$$

Hence, the slope of the $F(x)$ curve on semi-log paper gives the reciprocal of the mean lifetime. Furthermore, the centroid of $F(x)$ is displaced positively along the abscissa axis from the centroid of $\rho(x)$ by an amount $1/\lambda$, the mean lifetime. If the $F(x)$ and $\rho(x)$ curves are plotted to the same included area, then $F(x)$ and $\rho(x)$ rise from the same point on the left and intersect at the maximum of $F(x)$, provided $1/\lambda$ represents a single lifetime.

The slope of the curve may best be obtained using the method of least squares. In this method,[77] the slope is

$$\lambda = \frac{\Sigma N_i (c_i-\bar{c})(y_i-\bar{y})}{\Sigma N_i (c_i-\bar{c})} \qquad (7)$$

and the natural logarithm of the intercept is

$$b = \frac{\bar{y}\,\Sigma N_i c_i^2 - \bar{c}\,\Sigma N_i c_i y_i}{\Sigma (c_i - \bar{c})^2} \qquad (8)$$

where c_i is the channel number, N_i is the number of counts in channel c_i, and y_i equals $\ln_e N_i$. Furthermore, the variance in $1/\lambda$ is given by

$$\sigma_T = \frac{\tau^4}{\Sigma N_i (c_i - \bar{c})^2} \qquad (9)$$

These calculations were all performed on the IBM 650.

The percentage of positrons annihilating with a long lifetime is easily obtained once the $F(x)$ or τ_2 curve is found, as this is merely the ratio of the area of $F(x)$ to the area of the experimental composite curve. As an illustration, the above analysis will be applied to the data obtained for positrons annihilating in polyethylene at -98.5°C.

Starting with the prompt or aluminum curve, represented by a dashed line in Figure 21 (the ordinate is plotted as counts x 10^{-1} for clarity of illustration), that was obtained immediately after the polyethylene data, it is necessary to determine the centroid of the $P(x)$ curve: Summing the ordinates by Simpson's rule to get the area and taking moments about the zero point gives for the centroid:

$$\text{Centroid} = \frac{\text{Net moments}}{\text{Area}}$$

$$\text{Centroid} = \frac{468}{256} = 1.8 \text{ channels}$$

The "true zero" is now 1.8 channels to the right of the peak channel, minus the lifetime of positrons in aluminum. Using Bell and Jørgensen's[69]

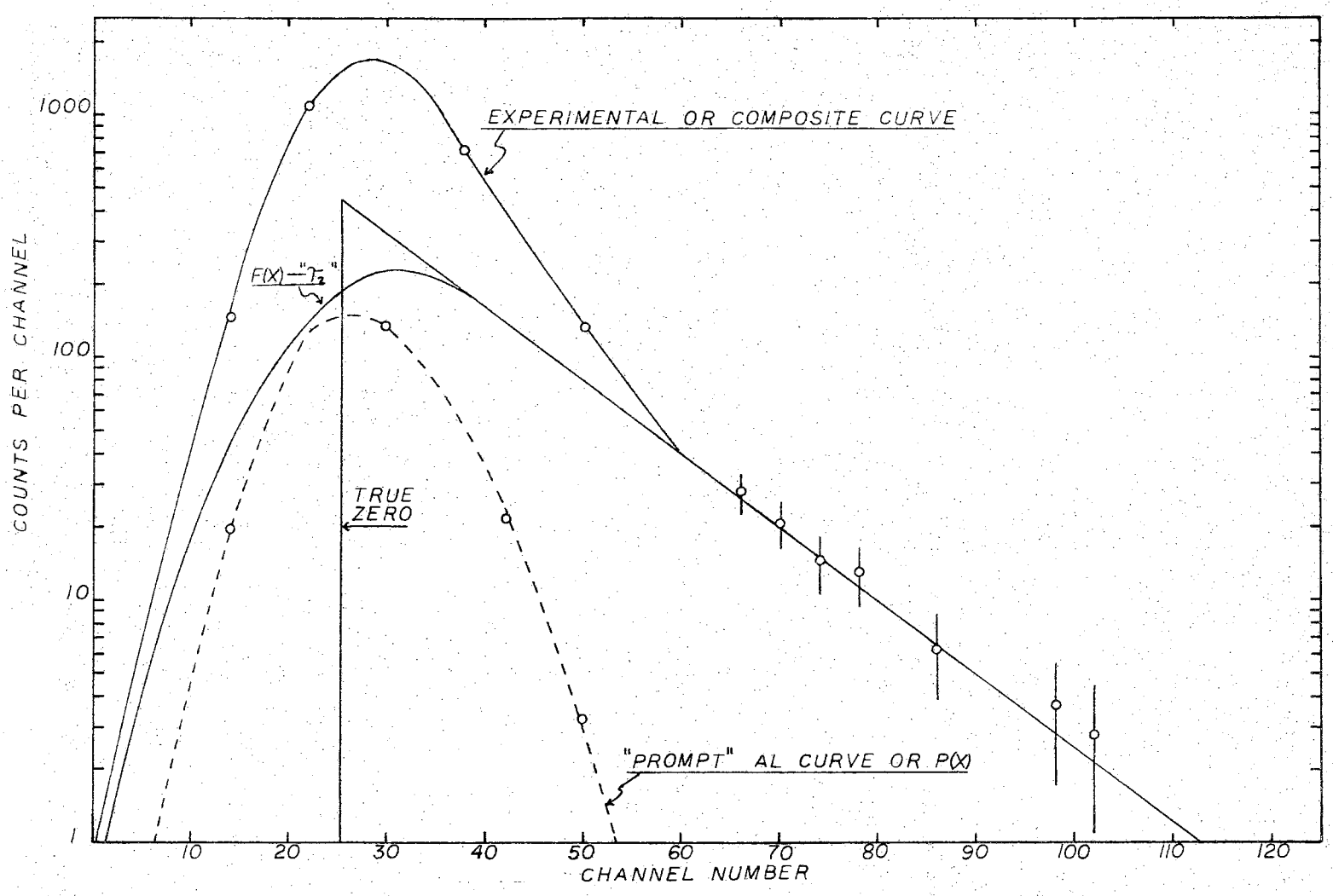

Figure 21. Sample Analysis Curve.

lifetime in aluminum value of $\tau_1 = 0.19$ ns. (which corresponds to 2.1 channels for this calibration), true zero is found to be 0.3 channels to the left of the peak channel. The values of $f(x)$ used in the folding process are now taken with respect to the "true zero" ordinate and are recorded in the second column of Table V. Once this is done, the tail or straight line portion of the polyethylene experimental curve (in the region where $F(x) \gg P(x)$) is extended back to the "true zero" point. The coordinates of the $e^{-\lambda t}$ are then recorded in the second row of Table V and are multiplied by the appropriate Simpson's rule constant, as illustrated in row three. The numerical integration is carried out by recording the product for each value of $P(x)$ with every value of $Ae^{-\lambda t}$ in the squares. Summation along the 45° Diagonals gives the values of $F(x)$ for the delayed curve to within a multiplicative constant. (It is actually not necessary to list each of these multiplications in the table if a desk calculator equipped with an accumulative multiply operation is available.) Since the multipliciative constant is not readily computable, the delayed curve is matched to the experimental curve in the region where the two curves are known to be equal, i.e., $F(x) \gg P(x)$.

The curve obtained by plotting the values of $F(x)$ on semi-logarithmic paper is then placed under the experimental composite curve so that the tails in the region of coincide, and the delayed curve is then drawn, giving the curves in Figure 21.

The areas of the delayed and composite curves are:

Area of $F(x) = 70.3 \times 10^2$ (In cts × channel)

Area of composite = 319×10^2 (In cts × channel)

The percentage of positrons annihilating with the long lifetime is

		t	0	5	10	15	20	25	30	35	40	45	50	55	60	65	70	75
		$e^{-\lambda t}$	490	310	200	166	110	74	54	38.6	27	19	13.5	9.4	6.6	4.7	3.3	2.4
X	P(x)	$Ae^{-\lambda t}$	817	2067	733	1107	367	507	190	257	40	127	50	62.7	30	31.3	11.	16
20	.8																	
15	5.4																	
10	29.5																	
5	99																	
0	148																	
-5	125																	
-10	70																	
-15	32																	
-20	10																	
-25	2.3		↓	↓	↓	↓	↓	↓	↓	↓	↓	↓	↓	↓	↓	↓	↓	↓	↓
		X	-25	-20	-15	-10	-5	0	5	10	15	20	25	30	35	40	45	50
		F(x)	18.8	129	485	1,332	2,882	4,709	5,713	5,199	3,916	2,827	1,949	1,373	941	689	487	352

Table 5. Sample Folding Process Calculation.

then $$\text{Percent of } \tau_2 = \frac{\text{Area } F(x)}{\text{Area Exp. Curve}} = \frac{70.3}{319} = 22\%$$

Centroid of $F(x) = 152$ channels $= 1.35$ ns.

It is worth noting that the least squares fit of the straight line portion (tail) of the experimental curve gave a value of 1.27 ns.

Subtracting the values of the τ_2 or $F(x)$ curve from the experimental (composite) curve gives the values for τ_1 (not shown in Figure 21). The τ_1 lifetime can be determined by centroid analysis. The value of τ_1 for this curve is 0.3 ns.

APPENDIX 3

TABLE VI

COMPLETE LIST OF RESULTS

Sample	Temp(°C)	τ_2 (R.M.S.) (ns.)	I_2 (%)	* τ_1 ($\times 10^{10}$ sec)	* τ_2 (Cent. Shift) (ns.)
Borax #1	23°C	.73 ± .07	37 ± 5	2.6	.63
Borax #3	23°C	1.19 ± .1	6 ± 5	1.4	1.3
Organic Wax	0°C	.97 ± .1	21 ± 5	1.1	.74
Organic Wax	23°C	1.31 ± .07	16 ± 5	3.4	.90
Organic Wax	80°C	1.99 ± .1	11 ± 5	1.7	1.8
Polyethylene	-195.8°C	1.08 ± .15	23 ± 5	2.3	1.1
Polyethylene	-78.5°C	1.27 ± .1	22 ± 5	3.4	1.4
Polyethylene	0.0°C	2.04 ± .1	12 ± 5	2.7	1.9
Polyethylene	23°C	2.60 ± .06	19 ± 5	2.0	2.2

*Error not quoted but felt to be rather large.

VITA

James Linville Pigg

Candidate for the Degree of

Master of Science

Thesis: VARIATION OF POSITRONIUM τ_2 LIFETIME WITH TEMPERATURE --ELECTRONIC SYSTEM OF MEASUREMENT.

Major Field: Physics

Biographical:

Personal Data: Born in Las Animas, Colorado, August 21, 1937, the son of Everett S. and Hester L. Pigg.

Education: Attended grade school in Las Animas, Colorado, and Sunnyside, Washington; graduated from Sunnyside Senior High School in 1955; received the Bachelor of Arts degree from Linfield College, McMinnville, Oregon, with a major in physics; completed the requirements for a Master of Science degree at Oklahoma State University in May 1962.

Professional Experience: Summer employment with Edgerton, Germeshausen, and Grier, Inc., Las Vegas, Nevada, 1957, 1958, and 1959 concerned with problems associated with prompt gamma detection.